References

Aloyz RS et al. (1998) p53 is essential for developmental neuron death as regulated by the TrkA and p75 neurotrophin receptors. J Cell Biol 143:1691–1703

Altaba ARi, Stecca B, Sanchez P (2004) Hedgehog-Gli signaling in brain tumors: stem cells and paradevelopmental programs in cancer. Cancer Lett 204:145–157

Axelson H (2004) The Notch signaling cascade in neuroblastoma: role of the basic helix-loop-helix proteins HASH-1 and HES-1. Cancer Lett 204:171–178

Azar CG, Scavarda NJ, Reynolds P, Brodeur GM (1990) Multiple defects of the nerve growth factor receptor in human neuroblastomas. Cell Growth Differ 1:421–428

Ball DW (2004) Achaete-scute homolog-1 and Notch in lung neuroendocrine development and cancer. Cancer Lett 159–169

Billon N et al. (2004) Roles for p53 and p73 during oligodendrocyte development. Development 131:1211–1220

Boon K et al. (2001) N-*MYC* enhances the expression of a large set of genes functioning in ribosome biogenesis and protein synthesis. EMBO J 20:1383–1393

Brodeur GM, Seeger RC, Schwab M, Varmus HE, Bishop JM (1984) Amplification of N-*MYC* in untreated human neuroblastomas correlates with advanced disease stage. Science 224:1121–1124

Canete A, Navarro S, Bermudez J, Pellin A, Castel V, Llombart-Bosch A (2000) Angiogenesis in neuroblastoma: relationship to survival and other prognostic factors in a cohort of neuroblastoma patients. J Clin Oncol 18:2789–2791

Deguin-Chambon V, Vacher M, Jullien M, May E, Bourdon JC (2000) Direct transactivation of c-Ha-Ras gene by p53: evidence for its involvement in p53 transactivation activity and p53-mediated apoptosis. Oncogene 19:5831–5841

Eggert A et al. (2000) Molecular dissection of TrkA signal transduction pathways mediating differentiation in human neuroblastoma cells. Oncogene 19:2043–2051

Eggert A et al. (2001) Resistance to tumor necrosis factor-related apoptosis-inducing ligand (TRAIL)-induced apoptosis in neuroblastoma cells correlates with a loss of caspase-8 expression. Cancer Res 61:1314–1319

El-Badry OM, Helman LJ, Chatten J, Steinberg SM, Evans AE, Israel MA (1991) Insulin-like growth factor II-mediated proliferation of human neuroblastoma. J Clin Invest 87: 648–657

Enomoto H et al. (1994) Identification of human DAN gene, mapping to the putative neuroblastoma tumor suppressor locus. Oncogene 9:2785–2791

Ernsberger U (2000) Evidence for an evolutionary conserved role of bone morphogenetic protein growth factors and phox2 transcription factors during noradrenergic differentiation of sympathetic neurons. Induction of a putative synexpression group of neurotransmitter-synthesizing enzymes. Eur J Biochem 267:6976–6981

Guillemot F, Lo LC, Johnson JE, Auerbach A, Anderson DJ, Joyner AL (1993) Mammalian achaete-scute homolog 1 is required for the early development of olfactory and autonomic neurons. Cell 75:463–476

Hamano S, Ohira M, Isogai E, Nakada K, Nakagawara A (2004) Identification of novel human neuronal leucine-rich repeat (hNLRR) family genes and inverse association of expression of Nbla10449/hNLRR-1 and Nbla10677/hNLRR-3 with the prognosis of primary neuroblastomas. Int J Oncol 24:1457–1466

Hishiki T et al. (1998) Glial cell line-derived neurotrophic factor/neurturin-induced differentiation and its enhancement by retinoic acid in primary human neuroblastomas expressing c-Ret, GFR-1 and GFR-2. Cancer Res 58:2158–2165

Huang EJ, Reichardt LF (2003) Trk receptors: roles in neuronal signal transduction. Annu Rev Biochem 72:609–642

Huber K, Combs S, Ernsberger U, Kalcheim C, Unsicker K (2002) Generation of neuroendocrine chromaffin cells from sympathoadrenal progenitors: beyond the glucocorticoid hypothesis. Ann NY Acad Sci 971:554–559

Hughes AL, Gollapudi L, Sladek TL, Neet KE (2000) Mediation of nerve growth factor-driven cell cycle arrest in PC12 cells by p53: simultaneous differentiation and proliferation subsequent to p53 functional inactivation. J Biol Chem 275: 37829–37837

Iavarone A, Lasorella A (2004) Id proteins in neural cancer. Cancer Lett 204:189–196

Ichikawa M, Murakumo Y, Takahashi M (2004) RET and neuroendocrine tumors. Cancer Lett 204:197–211

Ichimiya S et al (1999) p73 at chromosome 1p36.3 is lost in advanced stage neuroblastoma but its mutation is infrequent. Oncogene 18:1061–1066

Ichimiya S, Nimura Y, Seki N, Ozaki T, Nagase T, Nakagawara A (2001) Down-regulation of *hASH1* is associated with the retinoic acid-induced differentiation of human neuroblastoma cell lines. Med Pediatr Oncol 36:132–134

Ikeda H et al. (1995) Bcl-2 oncoprotein expression and apoptosis in neuroblastoma. J Pediatr Surg 30:805–808

Ikegaki N, Katsumata M, Tsujimoto Y, Nakagawara A, Brodeur GM (1995) Relationship between bcl-2 and *MYC* gene expression in human neuroblastoma. Cancer Lett 91:161–168

Islam A et al (2000) High expression of Survivin, mapped to 17q25, is significantly associated with poor prognostic factors and promotes cell survival in human neuroblastoma. Oncogene 19:617–623

Kadomatsu K, Muramatsu T (2004) Midkine and pleiotrophin in neural development and cancer. Cancer Lett 204:127–143

Kadomatsu K, Huang R-P, Suganuma T, Murata F, Muramatsu T (1990) A retinoic acid responsive gene MK found in the teratocarcinoma system is expressed in spatially and temporally controlled manner during mouse embryogenesis. J Cell Biol 110:607–616

Kawamoto T, Ohira M, Hamano S, Hori T, Nakagawara A (2003) High expression of the novel endothelin-converting enzyme genes, Nbla03145/ECEL1alpha and beta is associated with favorable prognosis in human neuroblastomas. Int J Oncol 22:815–822

Kitanaka C et al (2002) Increased Ras expression and caspase-independent neuroblastoma cell death: possible mechanism of spontaneous neuroblastoma regression. J Natl Cancer Inst 94:358–368

Klein R (1994) Role of neurotrophins in mouse neuronal development. FASEB J 8:738–744

Klesse LJ, Parada LF (1999) Trks: signal transduction and intracellular pathways. Microsc Res Tech 45:210–216

Kogner P, Barbany G, Dominici C, Castello MA, Raschella G, Persson H (1993) Coexpression of messenger RNA for TRK protooncogene and low affinity nerve growth factor receptor in neuroblastoma with favorable prognosis. Cancer Res 53:2044–2050

Lasorella A, Noseda M, Beyna M, Yokota Y, Iavarone A (2000) Id2 is a retinoblastoma protein target and mediates signalling by *MYC* oncoproteins. Nature 407:592–598

Laurenzi VD et al. (2000) Induction of neuronal differentiation by p73 in a neuroblastoma cell line. J Biol Chem 275: 15226–15231

Li Y-S et al. (1990) Cloning and expression of a developmentally regulated protein that induces mitogenic and neurite outgrowth activity. Science 250:1690–1694

Lo L, Morin X, Brunet JF, Anderson DJ (1999) Specification of neurotransmitter identity by Phox2 proteins in neural crest stem cells. Neuron 22:693–705

Mac SM, D'Cunha CA, Farnham PJ (2000) Direct recruitment of N-*MYC* to target gene promoters. Mol Carcinogr 29: 76–86

Massari ME, Murre C (2000) Helix-loop-helix proteins: regulators of transcription in eukaryotic organisms. Mol Cell Biol 20:429–440

Matsumoto K, Wada RK, Yamashiro JM, Kaplan DR, Thiele CJ (1995) Expression of brain-derived neurotrophic factor and $p145^{TrkB}$ affects survival, differentiation, and invasiveness of human neuroblastoma cells. Cancer Res 55:1798–1806

Moll UM, LaQuaglia M, Benard J, Riou G (1995) Wild-type p53 protein undergoes cytoplasmic sequestration in undifferentiated neuroblastomas but not in differentiated tumors. Proc Natl Acad Sci USA 92:4407–4411

Morin X, Cremer H, Hirsch MR, Kapur RP, Goridis C, Brunet JF (1997) Defects in sensory and autonomic ganglia and absence of locus coeruleus in mice deficient for the homeobox gene Phox2a. Neuron 18:411–423

Nakagawa T et al (2002) Autoinhibitory regulation of p73 by ΔNp73 to modulate cell survival and death through p73-specific target element within the ΔNp73 promoter. Mol Cell Biol 22:2575–2585

Nakagawara A (1998a) The NGF story and neuroblastoma. Med Pediatr Oncol 31:113–115

Nakagawara A (1998b) Molecular basis of spontaneous regression of neuroblastoma: role of neurotrophic signals and genetic abnormalities. Hum Cell 11:115–124

Nakagawara A (2001) Trk receptor tyrosine kinases: a bridge between cancer and neural development. Cancer Lett 169:107–114

Nakagawara A (2004) Neural crest development and neuroblastoma: the genetic and biological link. In: Aloe L, Calza L (eds) NGF and related molecules in health and disease. Elsevier, Amsterdam, pp 233–242

Nakagawara A, Arima M, Azar CG, Scavarda NJ, Brodeur GM (1992) Inverse relationship between trk expression and N-*MYC* amplification in human neuroblastomas. Cancer Res 52:1364–1368

Nakagawara A, Arima-Nakagawara M, Scavarda NJ, Azar CG, Cantor AB, Brodeur GM (1993) Association between high levels of expression of the TRK gene and favorable outcome in human neuroblastoma. N Engl J Med 328:847–854

Nakagawara A, Azar CG, Scavarda NJ, Brodeur GM (1994) Expression and function of TRK-B and BDNF in human neuroblastomas. Mol Cell Biol 14:759–767

Nakagawara A et al. (1995) Differential expression of pleiotrophin and midkine in advanced neuroblastomas. Cancer Res 55:1792–1797

Nakagawara A et al. (1997) High levels of expression and nuclear localization of ICE and CPP32 in favorable human neuroblastomas. Cancer Res 57:4578–4584

Nakamura Y, Ozaki T, Koseki H, Nakagawara A, Sakiyama S (2003) Accumulation of $p27^{KIP1}$ is associated with BMP2-mediated growth arrest and neuronal differentiation of human neuroblastoma-derived cell lines. Biochem Biophys Res Commun 307:206–213

Oppenheim RW (1991) Cell death during development of the nervous system. Annu Rev Neurosci 14:453–501

Pattyn A, Morin X, Cremer H, Goridis C, Brunet JF (1999) The homeobox gene Phox2b is essential for the development of autonomic neural crest derivatives. Nature 399:366–370

Pozniak CD, Radinovic S, Yang A, McKeon F, Kaplan DR, Miller FD (2000) An anti-apoptotic role for the p53 family member, p73, during developmental neuron death. Science 289:304–306

Radtke F, Raj K (2003) The role of Notch in tumorigenesis: oncogene or tumour suppressor? Nat Rev Cancer 3:756–767

Reale MA et al. (1996) Loss of DCC expression in neuroblastoma is associated with disease dissemination. Clin Cancer Res 2:1097–1102

Rodriguez-Leon J, Merino R, Macias D, Ganan Y, Santesteban E, Hurle JM (1999) Retinoic acid regulates programmed cell death through BMP signalling. Nat Cell Biol 1:125–126

Schneider C, Wicht H, Enderich J, Wegner M, Rohrer H (1999) Bone morphogenetic proteins are required in vivo for the generation of sympathetic neurons. Neuron 24:861–870

Schwab M et al. (1983) Amplified DNA with limited homology to *MYC* cellular oncogene is shared by human neuroblastoma cell lines and a neuroblastoma tumour. Nature 305:245–248

Schwab M et al (1984) Chromosome localization in normal human cells and neuroblastomas of a gene related to c-*MYC*. Nature 308:288–291

Schwab M et al. (2003) Neuroblastoma: biology and molecular and chromosomal pathology. Lancet Oncol 4:472–480

Schweigerer L, Ledoux D, Fleischmann G, Barritault D (1991) Enhanced *MYCN* oncogene expression in human neuroblastoma cells is associated with altered FGF receptor expression and cellular growth response to basic FGF. Biochem Biophys Res Commun 179:1449–1454

Seeger RC et al. (1985) Association of multiple copies of the N-*MYC* oncogene with rapid progression of neuroblastomas. N Engl J Med 313:1111–1116

Shinbo J et al. (2002) p73-dependent expression of DAN during cisplatin-induced cell death and osteoblast differentiation. Biochem Biophys Res Commun 295:501–507

Snider WD (1994) Functions of the neurotrophins during nervous system development: what the knockouts are teaching us. Cell 77:627–638

Soderholm H et al. (1999) Human achaete-scute homologue 1 (HASH-1) is downregulated in differentiating neuroblastoma cells. Biochem Biophys Res Commun 256:557–563

Stanke M, Junghans D, Geissen M, Goridis C, Ernsberger U, Rohrer H (1999) The Phox2 homeodomain proteins are sufficient to promote the development of sympathetic neurons. Development 126:4087–4094

Suzuki T, Bogenmann E, Shimada H, Stram D, Seeger RC (1993) Lack of high-affinity nerve growth factor receptors in aggressive neuroblastomas. J Natl Cancer Inst 85:377–384

Teitz T et al (2000) Caspase 8 is deleted or silenced preferentially in childhood neuroblastomas with amplification of *MYCN*. Nat Med 6:529–535

Tian H, Hammer RE, Matsumoto AM, Russell DW, McKnight SL (1998) The hypoxia-responsive transcription factor EPAS1 is essential for catecholamine homeostasis and protection against heart failure during embryonic development. Genes Dev 12:3320–3324

Trochet D et al (2004) Germline mutations of the paired-like homeobox 2B (PHOX2B) gene in neuroblastoma. Am J Hum Genet 74:761–764

Tweddle DA, Malcolm AJ, Bown N, Pearson AD, Lunec J (2001) Evidence for the development of p53 mutations after cytotoxic therapy in a neuroblastoma cell line. Cancer Res 61:8–13

Van Noesel MM, Pieters R, Voute PA, Versteeg R (2003) The N-*MYC* paradox: N-*MYC* overexpression in neuroblastomas is associated with sensitivity as well as resistance to apoptosis. Cancer Lett 197:165–172

Yamashiro D, Nakagawara A, Ikegaki N, Liu X, Brodeur GM (1996) Expression of TRK-C in favorable human neuroblastomas. Oncogene 12:37-41

Yang A, Walker N, Bronson R, Kaghad M, Oosterwegel M, Bonnin J, Vagner C, Bonnet H, Dikkes P, Sharpe A, McKeon F, Caput D (2000) p73-deficient mice have neurological, pheromonal and inflammatory defects but lack spontaneous tumours. Nature 404:99–103

Yano H, Cong F, Birge RB, Goff SP, Chao MV (2000) Association of the Abl tyrosine kinase with the Trk nerve growth factor receptor. J Neurosci Res 59:356–364

Yoshida I, Koide S, Nakagawara A, Tsuji A, Matsuda Y (2001) Proprotein convertase PACE4 is a target gene of the basic helix-loop-helix transcription factor hASH-1. Biochem J 360:683–689

British Journal of Cancer (2003) 88, 1522–1526

www.bjcancer.com

Correlation of elevated level of blood midkine with poor prognostic factors of human neuroblastomas

S Ikematsu[1,2], A Nakagawara[3], Y Nakamura[3], S Sakuma[4], K Wakai[5], T Muramatsu[1] and K Kadomatsu[*,1]

[1]Department of Biochemistry, Nagoya University Graduate School of Medicine, 65 Tsurumai-cho, Showaku, Nagoya 466-8550, Japan; [2]Pharmaceuticals Development Department, Meiji Dairies Co., Odawara 250-0862, Japan; [3]Division of Biochemistry, Chiba Cancer Center Research Institute, Chiba 260-8717, Japan; [4]Cell Signals Inc., Tokyo 101-0035, Japan; [5]Department of Preventive Medicine/Biostatistics and Medical Decision Making, Nagoya University Graduate School of Medicine, Nagoya 466-8550, Japan

The heparin-binding growth factor midkine (MK) is the product of a retinoic acid-responsive gene, and is implicated in neuronal survival and differentiation, and carcinogenesis. We previously reported that *MK* mRNA expression is elevated in neuroblastoma specimens at all stages, whereas pleiotrophin, the other member of the MK family, is expressed at high levels in favourable neuroblastomas. As MK is a secretory protein, it can be detected in the blood. Here, we show a significant correlation of the plasma MK level with prognostic factors of neuroblastomas. The plasma MK level was determined in 220 patients with neuroblastomas, and compared with that in children without malignant tumors ($n=17$, $<500\,pg\,ml^{-1}$). The plasma MK level became significantly elevated with advancing stages (stage 1: $445\,pg\,ml^{-1}$ (median), $n=73$; stage 2: 589, $n=39$; stage 3: 864, $n=40$; stage 4: 1445, $n=56$; and stage 4S: 2439, $n=12$). More importantly, a higher MK level was strongly correlated with poor prognostic factors: over 1 year of age ($P=0.0299$), *MYCN* amplification ($P<0.0001$), low *TrkA* expression ($P=0.0005$), nonmass screening, sporadic neuroblastomas ($P<0.0001$), and diploidy/tetraploidy ($P=0.0007$). Thus, these results demonstrate that the plasma MK level is a good marker for evaluating the progression of neuroblastomas. Moreover, considering the ability of antisense MK oligodeoxyribonucleotide to suppress tumour growth of colorectal carcinoma cells in nude mice, as recently reported, the present study suggests that MK is a possible candidate molecular target for therapy for neuroblastomas.
British Journal of Cancer (2003) **88**, 1522–1526. doi:10.1038/sj.bjc.6600938 www.bjcancer.com

Keywords: growth factor; midkine; molecular target; neuroblastoma; tumour marker

Midkine (MK) is a heparin-binding growth factor that was originally discovered as the product of a retinoic acid-responsive gene during the differentiation of embryonal carcinoma cells (Kadomatsu *et al*, 1988; Tomomura *et al*, 1990; Muramatsu, 2002). The MK family consists of only two members, namely MK and pleiotrophin (PTN; also called HB-GAM), and is distinct from other heparin-binding growth factor families (Kurtz *et al*, 1995; Rauvala *et al*, 2000; Deuel *et al*, 2002; Muramatsu, 2002). Regarding the biological roles of MK, at least three important issues should be pointed out. First, a pivotal role of MK in the migration of inflammatory cells has been revealed by studies involving MK knockout mice; MK-deficient mice are more resistant to vascular restenosis and nephritis induced by reperfusion (Horiba *et al*, 2000; Sato *et al*, 2001). Second, MK exhibits neuroprotective activity (Michikawa *et al*, 1993; Unoki *et al*, 1994; Owada *et al*, 1999), and enhances neurite extension (Muramatsu *et al*, 1993). Induction of MK expression has been detected in reactive astrocytes in ischaemic lesions in human and animal brains (Wang *et al*, 1998; Wada *et al*, 2002). MK is deposited at senile plaques and neurofibrillary tangles in Alzheimer's patients (Yasuhara *et al*, 1993). MK binds to Aβ and inhibits its cytotoxicity (Yu *et al*, 1998). Third, MK is involved in carcinogenesis. Its expression is induced as early as at the precancerous stages of human colorectal and prostate carcinomas (Konishi *et al*, 1999; Ye *et al*, 1999), increases with the stages of human carcinomas, and is significantly linked to the prognosis (O'Brien *et al*, 1996; Mishima *et al*, 1997). MK transforms NIH3T3 cells (Kadomatsu *et al*, 1997), enhances fibrinolysis (Kojima *et al*, 1995), and promotes cell growth (Muramatsu and Muramatsu, 1991; Muramatsu *et al*, 1993; Takei *et al*, 2001), cell survival (Qi *et al*, 2000), cell migration (Takada *et al*, 1997; Maeda *et al*, 1999; Horiba *et al*, 2000; Qi *et al*, 2001), and angiogenesis (Choudhuri *et al*, 1997). MK antisense oligodeoxyribonucleotide suppresses tumour progression in nude mice (Takei *et al*, 2001, 2002).

The neuroblastoma is the most common solid malignant tumour in children. However, the molecular mechanisms underlying its pathogenesis and progression remain unclear, although several molecules, such as MYCN, TrkA, and TrkB, that are linked to the prognosis have been revealed (Brodeur *et al*, 1984; Nakagawara *et al*, 1995). This is one of the reasons why satisfactorily efficient therapies have not been established yet. A possible approach regarding such therapies is to seek molecular targets in neuroblastomas. We previously reported that *MK* mRNA expression is elevated in neuroblastoma specimens at all stages (Nakagawara *et al*, 1995). Interestingly, the other MK family member, PTN, is expressed at high levels in favourable neuroblastomas (Nakagawara *et al*, 1995). As MK is a secretory

*Correspondence: Dr K Kadomatsu;
E-mail: kkadoma@med.nagoya-u.ac.jp
Received 27 November 2002; accepted 25 February 2003

protein, the blood MK level could be a strong tool for monitoring the status of neuroblastomas. This paper demonstrates that an elevated plasma level of MK is indeed significantly correlated with poor prognostic factors. Our results also indicate that MK could be a candidate molecular target for therapy for neuroblastomas.

MATERIALS AND METHODS

Enzyme-linked immunoassay for human MK

An enzyme-linked immunoassay (EIA) for human MK was performed as described previously (Ikematsu *et al*, 2000). Briefly, human MK was produced using *Pichia pastoris* GS115 by transfection with a human MK expression vector, which was constructed into pHIL-D4 (Invitrogen, Carlsbad, California, USA). This yeast-produced human MK was used to immunise rabbits and chickens to raise antibodies. The rabbit anti-human MK antibody (50 μl of 5.5 $\mu g\,ml^{-1}$ in 50 mM Tris HCl (pH 8.2), 0.15 M NaCl, 0.1% NaN_3) was coated onto the wells of microtitre plates (Polysorp plates, Nunc, Rochester, New York, USA) for 20 h at room temperature. After washing with 0.05% Tween 20 in PBS, the wells were blocked with 300 μl of 0.1% casein, 0.01% Microcide I (aMReSCO) in PBS for 20 h at 37°C. Plasma samples (10 μl each) were mixed with 100 μl of 50 mM Tris HCl (pH 8.4), 0.5 M KCl, 0.1% casein, 0.5% BSA, 0.01% Microcide I, and 0.1 $\mu g\,ml^{-1}$ peroxidase-labelled chicken anti-human MK antibody. Aliquots of 50 μl of this mixture were added to wells prepared as described above, and further subjected to chromogenic detection at OD_{450} using tetramethylbenzidine as the substrate. This EIA system shows linearity from 0 to 4 $ng\,ml^{-1}$ of MK, and there is no crossreaction with PTN (Ikematsu *et al*, 2000).

Plasma samples

Plasma samples were obtained from blood collected from outcome patients without malignant tumours ($n=17$) and neuroblastoma patients ($n=220$). The information is summarised in Table 1.

Table 1 Blood samples

	n
No malignant tumours	17
< 1 year	11
> 1 year	6
Neuroblastomas	220
Stage 1	73
Stage 2	39
Stage 3	40
Stage 4	56
Stage 4S	12
MYCN amplification −	176
MYCN amplification +	21
High *TrkA* expression	157
Low *TrkA* expression	53
Mass screening	122
Sporadic	82
Hyperdiploidy/pentaploidy	91
Diploidy/tetraploidy	119
< 1 year	154
> 1 year	52

Sum from each group number does not necessarily match the total number, because some information is missing for some individuals.

Statistics

For statistical analysis as to stages, the Kruskal–Wallis test was used to evaluate the statistical differences between groups. The Mann–Whitney *U*-test with Bonferroni's correction was used to further evaluate the difference between the two groups. For analysis as to other prognostic factors, the Mann–Whitney *U*-test was used. $P<0.05$ was taken to be statistically significant.

RESULTS

The plasma MK level increases with advancing stages

Plasma samples were collected from children without malignant tumours and neuroblastoma patients. The information on individuals and neuroblastomas is summarised in Table 1. Plasma from individuals without malignant tumours showed low levels of MK (116–483 $pg\,ml^{-1}$; median, 205) (Figure 1). These values are consistent with the data for sera from healthy adults (median, 154 $pg\,ml^{-1}$; cutoff value, 500 $pg\,ml^{-1}$) (Ikematsu *et al*, 2000). The EIA employed in the present study showed no difference between serum and plasma (data not shown). These results indicate that the plasma level of MK does not change with age, and that the cutoff value can be set as 500 $pg\,ml^{-1}$ for children.

The plasma MK level increased with advancing neuroblastoma stages. The median values were 445, 589, 864, 1445, and 2439 $pg\,ml^{-1}$ for stages 1, 2, 3, 4, and 4S, respectively (Figure 1). The percentages of patients showing MK levels of more than the cutoff value were 38.4, 59.0, 70.0, 83.9, and 91.7% for stages 1, 2, 3, 4, and 4S, respectively (Figure 1). The statistical significance is summarised in Table 2. Although stage 4S is included in the favourable neuroblastomas along with stages 1 and 2, the MK level was the highest at stage 4S among the stages. This may be interpreted as indicating that one of the parameters influencing the plasma MK level is the tumour volume.

An elevated plasma MK level is correlated with poor prognostic factors of neuroblastomas

The neuroblastoma is one of the best studied tumours. Several factors have been determined to be significantly linked to the prognosis. Cases with amplified *MYCN* show a poor prognosis (Brodeur *et al*, 1984). Low-level expression of the NGF receptor *Trk A* is linked to a poor prognosis (Nakagawara *et al*, 1993). Sporadic neuroblastomas show a worse outcome as compared with neuroblastomas detected by mass screening that is currently being carried out in Japan (Sawada, 1986). Neuroblastomas with diploidy or tetraploidy show a worse prognosis than those with hyperdiploidy or pentaploidy (Look *et al*, 1984). In addition, the outcome in patients of older than 1 year is worse compared with in patients of younger than 1 year (Fortner *et al*, 1968). All these prognostic factors were significantly correlated with a plasma MK level (Figure 2 and Table 3). A higher level of MK was correlated with *MYCN* amplification ($P<0.0001$), low expression of *TrkA* ($P=0.0005$), sporadic neuroblastomas ($P<0.0001$), diploidy/tetraploidy ($P=0.0007$), and older age ($P=0.0299$).

DISCUSSION

This study demonstrated that the plasma MK level is significantly correlated with prognostic factors of human neuroblastomas. The only exception was that the plasma MK level was the highest at stage 4S among the stages, although stage 4S belongs to the favourable group of neuroblastomas. Stage 4S is a special type of stage 4. Tumours at stage 4S show spontaneous regression (Evans *et al*, 1976). Before spontaneous regression, stage 4S exhibits large tumours and metastasis to the liver, bone marrow, and skin. We

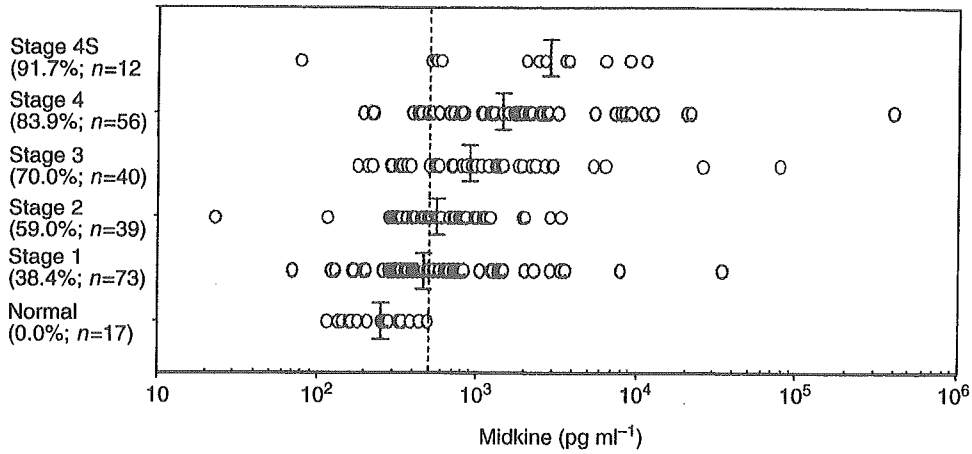

Figure 1 The plasma MK level becomes elevated with advancing neuroblastoma stages. The plasma MK level in children without malignant tumours was 205 pg ml^{-1} (median, $n=17$). Those at stages 1, 2, 3, 4, and 4S were 445 ($n=73$), 589 ($n=39$), 864 ($n=40$), 1445 ($n=50$), and 2439 ($n=12$), respectively. The percentage of cases showing more than the cutoff value (500 pg ml^{-1}) is shown in parentheses beneath each stage. The plasma MK level is significantly elevated at all neuroblastoma stages compared with the normal level. Statistical analysis is summarised in Table 2.

Table 2 Statistical analysis as to stages

Stage	Normal	Stage 1	Stage 2	Stage 3	Stage 4
1	<0.001				
2	<0.001	0.5<			
3	<0.001	0.039	0.5<		
4	<0.001	<0.001	<0.001	0.5<	
4S	0.003	0.001	0.067	0.5<	0.5<

The difference in serum MK level between the six groups was statistically significant ($P<0.0001$, by the Kruskal–Wallis test). *P*-values in this table for differences between the two groups were derived from the Mann–Whitney *U*-test with Bonferroni's correction.

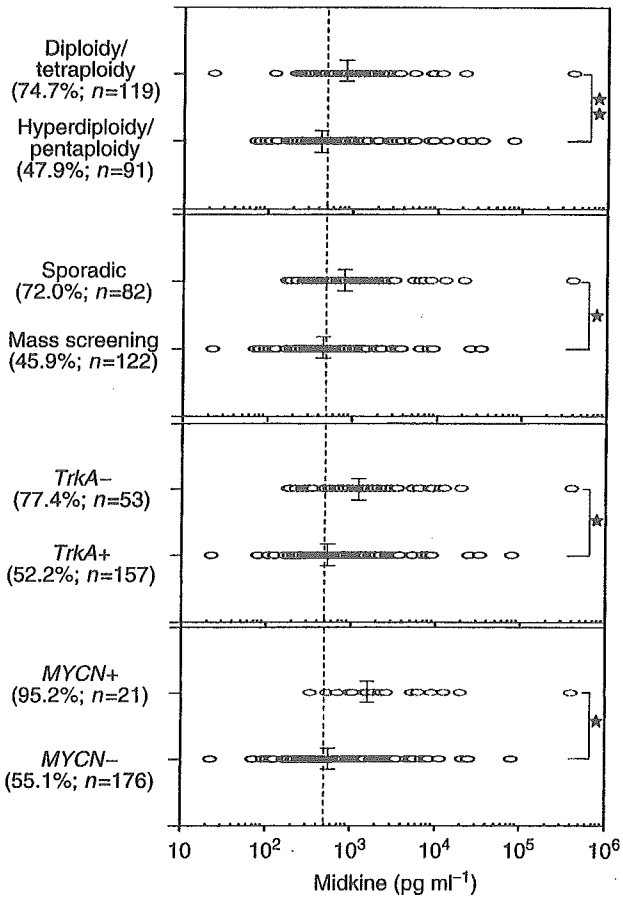

Figure 2 Correlation of the plasma MK level with several prognostic factors of neuroblastomas. Single asterisk, $P=0.0005$ or less; double asterisk, $P=0.0007$. The percentage of cases showing more than the cutoff value (500 pg ml^{-1}) is shown in parentheses. Statistical analysis is summarised in Table 3.

previously reported that MK mRNA expression in tumour specimens is very high at all human neuroblastoma stages, including stage 4S, as compared with that in benign tumours, that is, ganglioneuromas (Nakagawara *et al*, 1995). The present data for plasma MK are, therefore, consistent with our previous data for mRNA expression in tumours. Taken together, the results for stage 4S suggest that the tumour volume is one of the factors that influence the plasma MK level. However, the tumour volume may not be the only factor that controls the plasma MK level, because we detected many cases that showed a high MK level even at stage 1 (Figure 1). In favourable neuroblastomas, for example, no *MYCN* amplification was discovered by mass screening, and we often observed high MK plasma levels. It should be noted that, even in favourable neuroblastomas, many cases exhibit poor clinical courses. We can expect that such cases can be evaluated and managed by means of monitoring the plasma level of MK. The importance of the present study is that it provided a chance to follow up prognosis of the patients with several parameters, including the plasma MK level. This perspective study is currently being carried out by our group, which will reveal the biological and clinical significance of an elevated plasma level of MK.

The present results also indicated that MK could be a candidate molecular target for therapy for neuroblastomas, because an elevated plasma MK level is linked with a poor prognosis. Cancer-related activities of MK have been reported by many laboratories. These activities include transforming, migrating, fibrinolytic, mitogenic, antiapoptotic, and angiogenic ones (Kojima *et al*, 1995; Choudhuri *et al*, 1997; Kadomatsu *et al*, 1997; Qi *et al*, 2000, 2001). Furthermore, we recently succeeded in suppressing tumour growth by using antisense MK oligodeoxyribonucleotide (Takei *et al*, 2001, 2002). Thus, ablation of MK production or disruption of its signalling pathway could be a strong means of curing neuroblastomas. Regarding the signalling pathway of MK, receptor-type protein tyrosine phosphatase ζ, anaplastic leukaemia

Table 3 Statistical analysis as to several prognostic factors

MYCN amplification + *vs* −	<0.0001
TrkA expression low *vs* high	0.0005
Sporadic *vs* mass screening	<0.0001
Diploidy/tetraploidy *vs* hyperdiploidy/pentaploidy	0.0007
1 year< *vs* 1 year>	0.0299

Statistical analysis was performed using the Mann–Whitney *U*-test.

kinase, and LDL receptor-related protein (LRP) were recently identified as MK receptors (Maeda *et al*, 1999; Muramatsu *et al*, 2000; Stoica *et al*, 2002). Although it has not been elucidated yet whether or not these receptors form complexes for MK signalling, each protein serves as a receptor transducing intracellular signals for midkine. Further investigation of the MK action mechanism should provide insights as to a therapeutic strategy against aggressive neuroblastomas.

A recent report that 13-*cis*-retinoic acid could be a curative reagent for neuroblastomas (Matthay *et al*, 1999) prompted us to examine the effect of this reagent on MK production, because MK overproduction should make the prognosis worse if 13-*cis*-retinoic acid induced MK production. All-*trans*-retinoic acid as well as 13-*cis*-retinoic acid induced the intracellular production of MK, but did not enhance the secretion of MK, probably because of premature binding, as described below (manuscript in preparation). The endocytosis of MK is completely dependent on LRP, and initiates nuclear targeting by MK, which is partly needed for the antiapoptotic activity of MK (Shibata *et al*, 2002). In addition, LRP functions as a biosynthesis regulator for MK. Overexpression of MK leads to premature binding and aggregation of MK and LRP in the endoplasmic reticulum during the biosynthesis of both proteins, thus preventing MK overproduction that might cause overgrowth or transformation of cells (manuscript in preparation). Taken together, the present results suggest that MK production during tumour development needs enhancing mechanisms at least at two steps: mRNA expression and protein secretion.

One of the characteristics of MK expression is that it is frequently and highly expressed in malignant tumours regardless of the tissue type. This phenomenon is reminiscent of mutations in the p53 gene. We previously reported that an elevated serum MK level was detected in more than 80% frequency of human adult carcinomas (Ikematsu *et al*, 2000). Thus, monitoring of the level of the blood MK is applicable not only to neuroblastomas but also to adult carcinomas. Further assessment of the blood MK level with regard to tumour stages and prognosis of adult malignancy will provide indications for the use of blood MK as a tumour marker for each disease.

ACKNOWLEDGEMENTS

This work was supported by Grants-in-Aid from the Ministry of Education, Science, Sports, and Culture of Japan, and Grants-in-Aid for Center of Excellence Research.

REFERENCES

Brodeur GM, Seeger RC, Schwab M, Varmus HE, Bishop JM (1984) Amplification of N-myc in untreated human neuroblastomas correlates with advanced disease stage. *Science* **224:** 1121–1124

Choudhuri R, Zhang HT, Donnini S, Ziche M, Bicknell R (1997) An angiogenic role for the neurokines midkine and pleiotrophin in tumorigenesis. *Cancer Res* **57:** 1814–1819

Deuel TF, Zhang N, Yeh HJ, Silos-Santiago I, Wang ZY (2002) Pleiotrophin: a cytokine with diverse functions and a novel signaling pathway. *Arch Biochem Biophys* **397:** 162–171

Evans AE, Gerson J, Schnaufer L (1976) Spontaneous regression of neuroblastoma. *Natl Cancer Inst Monogr* **44:** 49–54

Fortner J, Nicastri A, Murphy ML (1968) Neuroblastoma: natural history and results of treating 133 cases. *Ann Surg* **167:** 132–142

Horiba M, Kadomatsu K, Nakamura E, Muramatsu H, Ikematsu S, Sakuma S, Hayashi K, Yuzawa Y, Matsuo S, Kuzuya M, Kaname T, Hirai M, Saito H, Muramatsu T (2000) Neointima formation in a restenosis model is suppressed in midkine-deficient mice. *J Clin Invest* **105:** 489–495

Ikematsu S, Yano A, Aridome K, Kikuchi M, Kumai H, Nagano H, Okamoto K, Oda M, Sakuma S, Aikou T, Muramatsu H, Kadomatsu K, Muramatsu T (2000) Serum midkine levels are increased in patients with various types of carcinomas. *Br J Cancer* **83:** 701–706

Kadomatsu K, Hagihara M, Akhter S, Fan QW, Muramatsu H, Muramatsu T (1997) Midkine induces the transformation of NIH3T3 cells. *Br J Cancer* **75:** 354–359

Kadomatsu K, Tomomura M, Muramatsu T (1988) cDNA cloning and sequencing of a new gene intensely expressed in early differentiation stages of embryonal carcinoma cells and in mid-gestation period of mouse embryogenesis. *Biochem Biophys Res Commun* **151:** 1312–1318

Kojima S, Muramatsu H, Amanuma H, Muramatsu T (1995) Midkine enhances fibrinolytic activity of bovine endothelial cells. *J Biol Chem* **270:** 9590–9596

Konishi N, Nakamura M, Nakaoka S, Hiasa Y, Cho M, Uemura H, Hirao Y, Muramatsu T, Kadomatsu K (1999) Immunohistochemical analysis of midkine expression in human prostate carcinoma. *Oncology* **57:** 253–257

Kurtz A, Schulte AM, Wellstein A (1995) Pleiotrophin and midkine in normal development and tumor biology. *Crit Rev Oncog* **6:** 151–177

Look AT, Hayes FA, Nitschke R, McWilliams NB, Green AA (1984) Cellular DNA content as a predictor of response to chemotherapy in infants with unresectable neuroblastoma. *N Engl J Med* **311:** 231–235

Maeda N, Ichihara-Tanaka K, Kimura T, Kadomatsu K, Muramatsu T, Noda M (1999) A receptor-like protein-tyrosine phosphatase PTPζ/RPTPβ binds a heparin-binding growth factor midkine. Involvement of arginine 78 of midkine in the high affinity binding to PTPζ. *J Biol Chem* **274:** 12474–12479

Matthay KK, Villablanca JG, Seeger RC, Stram DO, Harris RE, Ramsay NK, Swift P, Shimada H, Black CT, Brodeur GM, Gerbing RB, Reynolds CP (1999) Treatment of high-risk neuroblastoma with intensive chemotherapy, radiotherapy, autologous bone marrow transplantation, and 13-*cis*-retinoic acid. Children's Cancer Group. *N Engl J Med* **341:** 1165–1173

Michikawa M, Kikuchi S, Muramatsu H, Muramatsu T, Kim SU (1993) Retinoic acid responsive gene product, midkine, has neurotrophic functions for mouse spinal cord and dorsal root ganglion neurons in culture. *J Neurosci Res* **35:** 530–539

Mishima K, Asai A, Kadomatsu K, Ino Y, Nomura K, Narita Y, Muramatsu T, Kirino T (1997) Increased expression of midkine during the progression of human astrocytomas. *Neurosci Lett* **233:** 29–32

Muramatsu H, Muramatsu T (1991) Purification of recombinant midkine and examination of its biological activities: functional comparison of new heparin binding factors. *Biochem Biophys Res Commun* **177:** 652–658

Muramatsu H, Shirahama H, Yonezawa S, Maruta H, Muramatsu T (1993) Midkine, a retinoic acid-inducible growth/differentiation factor: immunochemical evidence for the function and distribution. *Dev Biol* **159:** 392–402

Muramatsu H, Zou K, Sakaguchi N, Ikematsu S, Sakuma S, Muramatsu T (2000) LDL receptor-related protein as a component of the midkine receptor. *Biochem Biophys Res Commun* **270:** 936–941

Muramatsu T (2002) Midkine and pleiotrophin: two related proteins involved in development, survival, inflammation and tumorigenesis. *J Biochem* **132:** 359–371

Nakagawara A, Arima-Nakagawara M, Scavarda NJ, Azar CG, Cantor AB, Brodeur GM (1993) Association between high levels of expression of the TRK gene and favorable outcome in human neuroblastoma. *N Engl J Med* **328:** 847–854

Nakagawara A, Milbrandt J, Muramatsu T, Deuel TF, Zhao H, Cnaan A, Brodeur GM (1995) Differential expression of pleiotrophin and midkine in advanced neuroblastomas. *Cancer Res* **55:** 1792–1797

O'Brien T, Cranston D, Fuggle S, Bicknell R, Harris AL (1996) The angiogenic factor midkine is expressed in bladder cancer, and overexpression correlates with a poor outcome in patients with invasive cancers. *Cancer Res* **56:** 2515–2518

Owada K, Sanjo N, Kobayashi T, Mizusawa H, Muramatsu H, Muramatsu T, Michikawa M (1999) Midkine inhibits caspase-dependent apoptosis via the activation of mitogen-activated protein kinase and phosphatidylinositol 3-kinase in cultured neurons. *J Neurochem* **73:** 2084–2092

Qi M, Ikematsu S, Ichihara-Tanaka K, Sakuma S, Muramatsu T, Kadomatsu K (2000) Midkine rescues Wilms' tumor cells from cisplatin-induced apoptosis: regulation of bcl-2 expression by midkine. *J Biochem* **127:** 269–277

Qi M, Ikematsu S, Maeda N, Ichihara-Tanaka K, Sakuma S, Noda M, Muramatsu T, Kadomatsu K (2001) Haptotactic migration induced by midkine. Involvement of protein-tyrosine phosphatase ζ. Mitogen-activated protein kinase, and phosphatidylinositol 3-kinase. *J Biol Chem* **276:** 15868–15875

Rauvala H, Huttunen HJ, Fages C, Kaksonen M, Kinnunen T, Imai S, Raulo E, Kilpelainen I (2000) Heparin-binding proteins HB-GAM (pleiotrophin) and amphoterin in the regulation of cell motility. *Matrix Biol* **19:** 377–387

Sato W, Kadomatsu K, Yuzawa Y, Muramatsu H, Hotta N, Matsuo S, Muramatsu T (2001) Midkine is involved in neutrophil infiltration into the tubulointerstitium in ischemic renal injury. *J Immunol* **167:** 3463–3469

Sawada T (1986) Outcome of 25 neuroblastomas revealed by mass screening in Japan. *Lancet* **1:** 377

Shibata Y, Muramatsu T, Hirai M, Inui T, Kimura T, Saito H, McCormick LM, Bu G, Kadomatsu K (2002) Nuclear targeting by the growth factor midkine. *Mol Cell Biol* **22:** 6788–6696

Stoica GE, Kuo A, Powers C, Bowden ET, Sale EB, Riegel AT, Wellstein A (2002) Midkine binds to anaplastic lymphoma kinase (ALK) and acts as a growth factor for different cell types. *J Biol Chem* **277:** 35990–35998

Takada T, Toriyama K, Muramatsu H, Song XJ, Torii S, Muramatsu T (1997) Midkine, a retinoic acid-inducible heparin-binding cytokine, in inflammatory responses: chemotactic activity to neutrophils and association with inflammatory synovitis. *J Biochem* **122:** 453–458

Takei Y, Kadomatsu K, Itoh H, Sato W, Nakazawa K, Kubota S, Muramatsu T (2002) 5′-, 3′-inverted thymidine-modified antisense oligodeoxynucleotide targeting midkine. Its design and application for cancer therapy. *J Biol Chem* **277:** 23800–23806

Takei Y, Kadomatsu K, Matsuo S, Itoh H, Nakazawa K, Kubota S, Muramatsu T (2001) Antisense oligodeoxynucleotide targeted to Midkine, a heparin-binding growth factor, suppresses tumorigenicity of mouse rectal carcinoma cells. *Cancer Res* **61:** 8486–8491

Tomomura M, Kadomatsu K, Matsubara S, Muramatsu T (1990) A retinoic acid-responsive gene, MK, found in the teratocarcinoma system. Heterogeneity of the transcript and the nature of the translation product. *J Biol Chem* **265:** 10765–10770

Unoki K, Ohba N, Arimura H, Muramatsu H, Muramatsu T (1994) Rescue of photoreceptors from the damaging effects of constant light by midkine, a retinoic acid responsive gene product. *Invest Opthalmol Vis Sci* **35:** 4063–4068

Wada M, Kamata M, Aizu Y, Morita T, Hu J, Oyanagi K (2002) Alteration of midkine expression in the ischemic brain of humans. *J Neurol Sci* **200:** 67–73

Wang S, Yoshida Y, Goto M, Moritoyo T, Tsutsui J, Izumo S, Sato E, Muramatsu T, Osam M (1998) Midkine exists in astrocytes in the early stage of cerebral infarction. *Brain Res Dev Brain Res* **106:** 205–209

Yasuhara O, Muramatsu H, Kim SU, Muramatsu T, Maruta H, McGeer PL (1993) Midkine, a novel neurotrophic factor, is present in senile plaques of Alzheimer disease. *Biochem Biophys Res Commun* **192:** 246–251

Ye C, Qi M, Fan QW, Ito K, Akiyama S, Kasai Y, Matsuyama M, Muramatsu T, Kadomatsu K (1999) Expression of midkine in the early stage of carcinogenesis in human colorectal cancer. *Br J Cancer* **79:** 179–184

Yu GSP, Hu J, Nakagawa H (1998) Inhibition of β-amyloid cytotoxicity by midkine. *Neurosci Lett* **254:** 125–128

THE JOURNAL OF BIOLOGICAL CHEMISTRY
Vol. 279, No. 12, Issue of March 19, pp. 11327–11335, 2004
Printed in U.S.A.

NEDL1, a Novel Ubiquitin-protein Isopeptide Ligase for Dishevelled-1, Targets Mutant Superoxide Dismutase-1*

Received for publication, November 12, 2003, and in revised form, December 16, 2003
Published, JBC Papers in Press, December 18, 2003, DOI 10.1074/jbc.M312389200

Kou Miyazaki‡, Tomoyuki Fujita‡, Toshinori Ozaki‡, Chiaki Kato‡, Yuka Kurose‡, Maya Sakamoto‡, Shinsuke Kato§, Takeshi Goto¶, Yasuto Itoyama‖, Masashi Aoki‖, and Akira Nakagawara‡

From the ‡Division of Biochemistry, Chiba Cancer Center Research Institute, Chiba 260-8717, Japan, the §Division of Neuropathology, Institute of Neurological Sciences, Faculty of Medicine, Tottori University, Yonago 683-8504, Japan, ¶Hisamitsu Pharmaceutical Company Incorporated, Tokyo 100-622, Japan, and the ‖Department of Neurology, Tohoku University School of Medicine, Sendai 980-8574, Japan

Approximately 20% of familial amyotrophic lateral sclerosis (FALS) arises from germ-line mutations in the superoxide dismutase-1 (*SOD1*) gene. However, the molecular mechanisms underlying the process have been elusive. Here, we show that a neuronal homologous to E6AP carboxyl terminus (HECT)-type ubiquitin-protein isopeptide ligase (NEDL1) physically binds translocon-associated protein-δ and also binds and ubiquitinates mutant (but not wild-type) SOD1 proportionately to the disease severity caused by that particular mutant. Immunohistochemically, NEDL1 is present in the central region of the Lewy body-like hyaline inclusions in the spinal cord ventral horn motor neurons of both FALS patients and mutant *SOD1* transgenic mice. Two-hybrid screening for the physiological targets of NEDL1 has identified Dishevelled-1, one of the key transducers in the Wnt signaling pathway. Mutant SOD1 also interacted with Dishevelled-1 in the presence of NEDL1 and caused its dysfunction. Thus, our results suggest that an adverse interaction among misfolded SOD1, NEDL1, translocon-associated protein-δ, and Dishevelled-1 forms a ubiquitinated protein complex that is included in potentially cytotoxic protein aggregates and that mutually affects their functions, leading to motor neuron death in FALS.

Amyotrophic lateral sclerosis (ALS)[1] is a progressive, fatal, neurodegenerative disease that is characterized by selective loss of motor neurons in the spinal cord, brain stem, and motor cortex. The sporadic and familial forms of the disease have similar clinical and pathological features. About 10% of ALS cases are familial, and mutation of superoxide dismutase-1 (SOD1) is found in 20% of familial ALS (FALS) patients (1, 2). Mice that express mutant *SOD1* transgenes develop an age-dependent ALS phenotype independent of levels of dismutase activity, suggesting that FALS pathology is because of a toxic gain of function in SOD1 and that the abnormal protein structure of mutant SOD1 is critical in the pathogenesis of motor neuron death (3–6). Recently, proteasome expression and activity have been reported to decrease with age in the spinal cord (7, 8). Furthermore, mutant SOD1 turns over more rapidly than wild-type SOD1, and an inhibitor of proteasome action inhibits this turnover and thus selectively increases the steady-state level of mutant SOD1 (8). These results suggest the involvement of the ubiquitin-proteasome function in the cause of FALS. However, the biochemical nature of this gain-of-function mutation in SOD1 and the mechanism by which SOD1 mutations cause the degeneration of motor neurons have remained elusive.

We show here the identification of a novel HECT-type ubiquitin-protein isopeptide ligase (E3), NEDL1, which is expressed in neuronal tissues, including the spinal cord, and selectively binds to and ubiquitinates mutant (but not wild-type) SOD1. NEDL1 is physically associated with translocon-associated protein-δ (TRAP-δ), one of the endoplasmic reticulum (ER) translocon components that has previously been reported to bind mutant SOD1 (9, 10). Both NEDL1 and TRAP-δ form a complex with mutant SOD1, with the binding intensity among these proteins being roughly proportionate to the rapidity of progression of the associated FALS phenotype. Immunohistochemical study has shown that NEDL1 is positive in the Lewy body-like hyaline inclusions in the spinal cord motor neurons of both FALS patients and mutant *SOD1* transgenic mice. We have also found that NEDL1 targets Dishevelled-1 (Dvl1) for ubiquitination-mediated degradation and that mutant (but not wild-type) SOD1 affects the function of Dvl1. Our observations suggest that NEDL1 is a quality control E3 that recognizes mutant SOD1 to form a tight complex with the physiological targets of NEDL1 in motor neurons of FALS patients.

EXPERIMENTAL PROCEDURES

Cell Culture and Transfection—Human neuroblastoma-derived cells were grown in RPMI 1640 medium supplemented with 10% heat-inactivated fetal bovine serum, 100 units/ml penicillin, and 100 μg/ml streptomycin. COS-7 and Neuro2a cells were maintained in Dulbecco's modified Eagle's medium supplemented with 10% heat-inactivated fe-

* This work was supported in part by Hisamitsu Pharmaceutical Co. Inc. (to A. N.), by grants from the Ministry of Health, Labor, and Welfare of Japan (to A. N. and Y. I.), and by grants from the Ministry of Education, Culture, Sports, Science, and Technology of Japan (to A. N., Y. I., and M. A.). The costs of publication of this article were defrayed in part by the payment of page charges. This article must therefore be hereby marked "*advertisement*" in accordance with 18 U.S.C. Section 1734 solely to indicate this fact.

The nucleotide sequence(s) reported in this paper has been submitted to the GenBank™/EBI Data Bank with accession number(s) AB048365 (Nbla0078 and human NEDL1), AB002320 (KIAA0322), and AB083710 (mouse Nedl1).

** To whom correspondence should be addressed: Div. of Biochemistry, Chiba Cancer Center Research Inst., 666-2 Nitona, Chuoh-ku, Chiba 260-8717, Japan. Tel.: 81-43-264-5431; Fax: 81-43-265-4459; E-mail: akiranak@chiba-ccri.chuo.chiba.jp.

[1] The abbreviations used are: ALS, amyotrophic lateral sclerosis; FALS, familial amyotrophic lateral sclerosis; SOD1, superoxide dismutase-1; E3, ubiquitin-protein isopeptide ligase; NEDL1, NEDD4-like ubiquitin-protein ligase-1; TRAP-δ, translocon-associated protein-δ; ER, endoplasmic reticulum; Dvl1, Dishevelled-1; RT, reverse transcription; LBHI, Lewy body-like hyaline inclusion; JNK, c-Jun N-terminal kinase; HECT domain, homologous to E6AP carboxyl-terminus.

tal bovine serum, 100 units/ml penicillin, and 100 μg/ml streptomycin. All cells were maintained in a humidified 37 °C incubator with 5% CO_2. All transfections were carried out with LipofectAMINE Plus transfection reagent (Invitrogen) according to the manufacturer's instructions. In some experiments, transfected cells were treated with MG-132 for 30 min at a final concentration of 40 μM.

RNA Analysis—A human multiple tissue mRNA blot and a fetal human multiple mRNA blot (Invitrogen) were hybridized with a ^{32}P-labeled ApaI-ScaI restriction fragment of *NEDL1* cDNA under standard conditions. For reverse transcription (RT)-PCR analysis, cDNA derived from adult human neural system (BioChain Institute, Hayward, CA) was subjected to PCR amplification using the following primers: *NEDL1*, 5′-CCGATTTGAGATCACTTCCTCC-3′ (sense) and 5′-CCGCTTTCCATCAGGTTGTT-3′ (antisense); and glyceraldehyde-3-phosphate dehydrogenase, 5′-ACCTGACCTGCCGTCTAGAA-3′ (sense) and 5′-TCCACCACCCTGTTGCTGTA-3′ (antisense). The amplified products were separated by electrophoresis on a 1.5% agarose gel and visualized by ethidium bromide post-staining. Amplification of glyceraldehyde-3-phosphate dehydrogenase was used as an internal control.

In Vitro Ubiquitination Assays—*In vitro* ubiquitination assays were performed as follows. Reaction mixtures containing 0.5 μg of purified glutathione *S*-transferase fusion proteins, 0.25 μg of yeast ubiquitin-activating enzyme (*E1*) (BostonBiochem, Cambridge, MA), 1 μl of crude lysates from *Escherichia coli* expressing ubiquitin carrier proteins (*E2*), and 10 μg of bovine ubiquitin (Sigma) were incubated in 250 mM Tris-HCl (pH 7.6), 1.2 M NaCl, 50 mM ATP, 10 mM $MgCl_2$, and 30 mM dithiothreitol. Reactions were terminated after 2 h at 30 °C by the addition of SDS sample buffer. Samples were resolved by SDS-PAGE, transferred to membranes, and immunoblotted with anti-ubiquitin monoclonal antibody 1B3 (Medical & Biological Laboratories, Nagoya, Japan).

Immunofluorescence Staining—Cells grown on coverslips were processed for immunofluorescence. Briefly, cells were fixed in 3.7% formaldehyde, permeabilized in 0.2% Triton X-100, and finally incubated with anti-NEDL1 antibody (diluted 1:100). The primary antibody was detected with fluorescein isothiocyanate-conjugated goat anti-rabbit IgG (diluted 1:500; Jackson ImmunoResearch Laboratories, Inc., West Grove, PA). Images were taken using an Olympus confocal microscopy system.

Yeast Two-hybrid Screening—Yeast two-hybrid screening was performed using the Gal4-based Matchmaker two-hybrid system with the cDNA libraries derived from fetal human brain (first screening) and adult human brain (second screening) (Clontech, Palo Alto, CA). *Saccharomyces cerevisiae* CG1945 cells were transformed with pAS2–1-NEDL1-1 (amino acids 757–1114; first screening) or pAS2–1-NEDL1-2 (amino acids 382–1448; second screening), which did not activate the transcription of *lacZ* alone. The transformants were subsequently transformed with the cDNA library, and the *lacZ*-positive colonies were selected. The plasmid DNAs were extracted from these positive colonies, and their nucleotide sequences were determined.

Immunoprecipitation and Western Blot Analysis—Anti-NEDL1 and anti-TRAP-δ polyclonal antibodies were raised in rabbits against an NEDL1 oligopeptide (amino acids 460–482) and a TRAP-δ oligopeptide (amino acids 93–126), respectively. For immunoprecipitation, COS-7 or Neuro2a cells were cotransfected with the expression plasmids in various combinations and lysed 48 h later in 10 mM Tris-HCl (pH 7.8), 150 mM NaCl, 1% Nonidet P-40, 1 mM EDTA, and 1 mM phenylmethylsulfonyl fluoride supplemented with protease inhibitor mixture (Sigma). Whole cell lysates were immunoprecipitated with anti-NEDL1, anti-FLAG (M2; Sigma), or anti-Myc (9B11; Cell Signaling Technology, Beverly, MA) antibody. Immune complexes were recovered on protein G-Sepharose beads, eluted by boiling in Laemmli sample buffer, electrophoresed on SDS-polyacrylamide gel, and then transferred to a polyvinylidene difluoride membrane (Immobilon, Millipore Corp., Bedford, MA) by electroblotting. For ubiquitination experiments, cell lysis was performed in radioimmune precipitation assay buffer (10 mM Tris-HCl (pH 7.4), 150 mM NaCl, 1% Nonidet P-40, 0.1% sodium deoxycholate, 0.1% SDS, and 1 mM EDTA), followed by strong sonication and freeze-thaw. The membrane was probed with the indicated primary antibodies and then incubated with the appropriate secondary antibodies labeled with horseradish peroxidase (Jackson ImmunoResearch Laboratories, Inc. and Southern Biotechnology Associates, Inc., Birmingham, AL). Immunoreactive bands were detected by the enhanced chemiluminescence technique (ECL, Amersham Biosciences). For the detection of c-Jun phosphorylation, we used anti-c-Jun (sc-45, Santa Cruz Biotechnology, Santa Cruz, CA) or anti-phospho-Ser^{63} c-Jun (Cell Signaling Technology) antibody.

Cloning of Human NEDL1 cDNA—A forward primer (5′-GGTTTTTAGGCCTGGCCGCC-3′) and a reverse primer (5′-CAATGAGGTACATGCCAATCC-3′) were used to amplify the 5′-part of the *NEDL1* cDNA using cDNA libraries derived from human neuroblastoma and fetal human brain (Stratagene, La Jolla, CA) as templates. The full-length human *NEDL1* cDNA was generated by fusion of the PCR-amplified fragment (nucleotides +1 to +68, where position +1 represents the translation initiation site) and the *KIAA0322* cDNA (a gift from T. Nagase, Kazusa DNA Institute). Gel electrophoresis and Western blot analysis were carried out as described above.

Expression Constructs—The mammalian expression plasmids for hemagglutinin-tagged and His_6-tagged ubiquitin were kind gifts of D. Bohmann. The full-length *NEDL1* cDNA was inserted into the mammalian expression plasmid pEF1/His (Invitrogen) or pIRESpuro2 (Clontech). cDNAs encoding wild-type and mutant forms of SOD1 were fused to the FLAG or Myc epitope tag sequence at their C termini and subcloned into pIRESpuro2. Similarly, the FLAG or Myc epitope tag sequence was attached to the C terminus of TRAP-δ. Also similarly, the FLAG or Myc epitope tag sequence was attached to the N terminus of Dvl1. Coding sequences were verified by automated DNA sequencing.

Protein Stability Experiments—Neuro2a cells were transfected with the expression plasmid for the wild-type or mutant form of SOD1 with or without the NEDL1 expression plasmid. Twenty-four hours after transfection, cycloheximide (50 μg/ml) was added to the culture medium, and the cells were harvested at the indicated time points by lysis in radioimmune precipitation assay buffer. The protein concentrations were determined using the Bradford protein assay system (Bio-Rad) according to the instructions of the manufacturer.

Immunohistochemistry—The immunohistochemical studies were performed as described previously using affinity-purified rabbit anti-NEDL1 antibody (11). Patient tissues were obtained at autopsy from two FALS siblings from a Japanese family. The clinical course of the sister, who died at age 46, was 18 months (case 1), and that of the brother, who died at age 65, was 11 years (case 2) (11). The *SOD1* gene was mutated with a 2-bp deletion at codon 126 (11, 12). Normal spinal cord tissues were obtained from three neurologically and neuropathologically normal individuals. The same study was performed on spinal cord tissues from three normal rats and a transgenic ALS rat carrying a mutant allele of the human *SOD1* gene (H46R) (13). These mice were killed at 180 days. As a negative control, some sections were incubated with anti-NEDL1 antibody that had been pre-absorbed with an excess of NEDL1 antigen. Bound antibodies were visualized by the avidin·biotin·immunoperoxidase complex method.

RESULTS

Cloning and Expression of the NEDL1 E3 Gene—To detect novel molecules that are important in regulating neuronal programmed cell death, we constructed oligo-capping cDNA libraries from a mixture of three fresh human neuroblastoma tissues (stages 1 and 2) that were undergoing gradual spontaneous regression, probably by neuronal apoptosis (14). Screening of 1152 novel genes by RT-PCR revealed that 194 genes were expressed differentially in regressing neuroblastomas with favorable prognosis and in aggressive tumors with poor prognosis. Among these genes, we found a partial cDNA sequence with an HECT-like domain (*Nbla0078*) that partially matched the *KIAA0322* gene. Because *KIAA0322* lacks a 5′-coding region, we used a genome-based PCR procedure to clone the corresponding full-length cDNA. This is predicted to encode a protein product of 1585 amino acids with homology to NEDD4 E3 (15, 16), which includes a C2 domain at the N-terminal region supposed to mediate its membrane localization in a calcium-dependent manner, two WW motifs important for protein-protein interaction through binding to specific proline-rich clusters, and a conserved catalytic HECT domain at the C terminus (Fig. 1*A*). We named this novel ligase, which mapped to chromosome 7p13, NEDL1 (NEDD4-like ubiquitin-protein ligase-1). We also cloned the mouse counterpart of *NEDL1* cDNA, whose amino acid sequence is 78% identical to the human sequence. Tissue-specific expression of *NEDL1* mRNA of ~10 and 7 kb in size was observed, with predominant expression in adult and fetal brains as examined by Northern blot analysis (Fig. 1*B*). Its

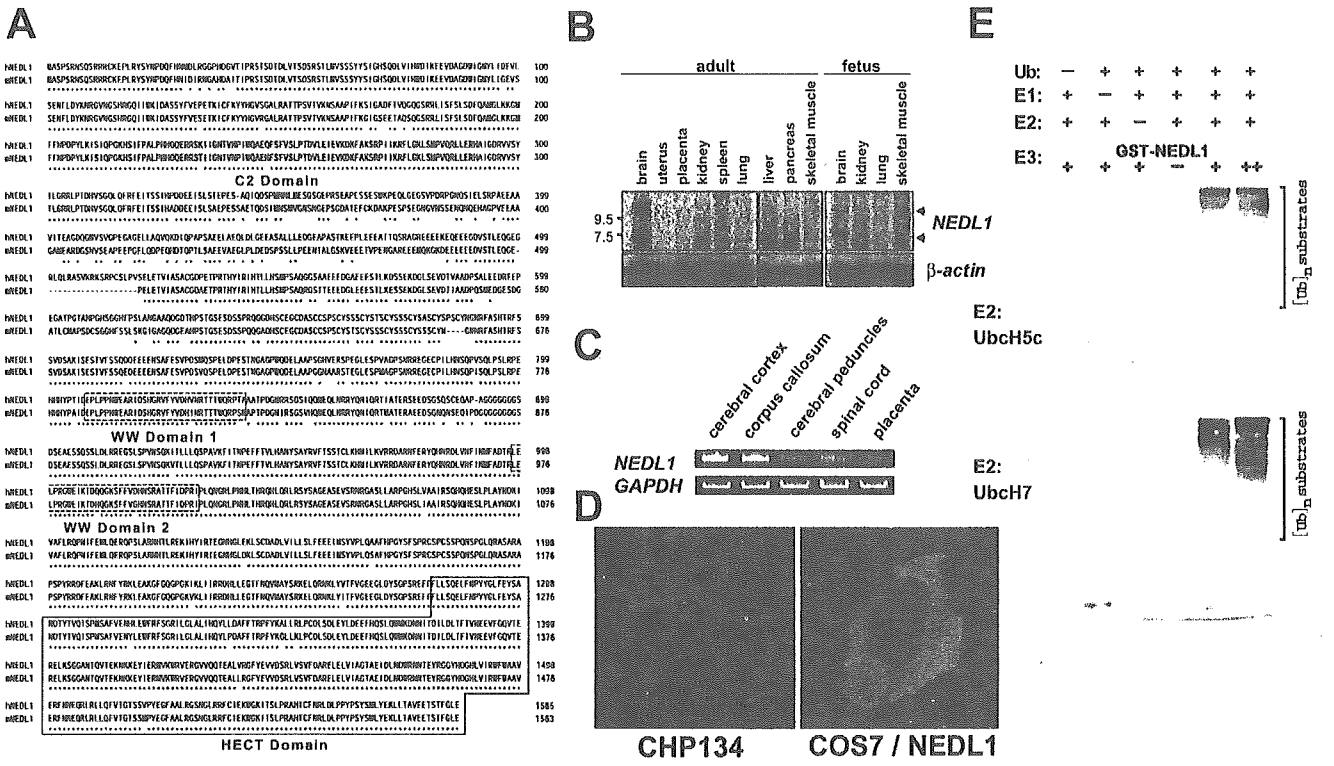

FIG. 1. **Amino acid sequence, brain-specific expression, and subcellular localization of NEDL1 E3.** *A*, alignment of conserved amino acid sequences of human NEDL1 (*hNEDL1*) and its mouse homolog (*mNEDL1*). *Numbers* on the right indicate the number of residues to the initiator methionine. The C2 domain (*shaded*), two WW domains (*dashed boxes*), and the HECT domain (*solid box*) are indicated. *B*, brain-specific expression of *NEDL1* mRNA. Total RNAs derived from the indicated adult (*left panel*) and fetal (*right panel*) human tissues were analyzed by Northern blotting using a ^{32}P-labeled human *NEDL1* cDNA restriction fragment as a probe. Control hybridization with a human β-actin cDNA probe verified the equal amount of RNA loaded. *C*, expression of *NEDL1* in human brain subsections. Total RNA from the cerebral cortex, corpus callosum, cerebral peduncles, spinal cord, or placenta was subjected to RT-PCR using specific primers for *NEDL1* or glyceraldehyde-3-phosphate dehydrogenase (*GAPDH*). RT-PCR analysis for *NEDL1* in the placenta provided a negative control. Amplification of glyceraldehyde-3-phosphate dehydrogenase was used as an internal control. *D*, confocal microscopic images of human neuroblastoma CHP134 cells (*left panel*) and COS-7 cells transfected with an expression plasmid for NEDL1 (*right panel*). Cells were subjected to immunofluorescence analysis using rabbit anti-NEDL1 polyclonal antibody, followed by fluorescein isothiocyanate-conjugated anti-mouse IgG. E, *in vitro* ubiquitination assays showing that NEDL1 has a ubiquitin-protein ligase activity. The degree of ubiquitination was increased in an NEDL1-dependent manner. In this assay, yeast ubiquitin-activating enzyme (*E1*), bacterially expressed ubiquitin carrier protein (*E2*; UbcH5C or UbcH7), and bacterial lysates were incubated in the presence or absence of increasing amounts of glutathione *S*-transferase (*GST*)-NEDL1. Polyubiquitinated bacterial proteins appeared to migrate in a high molecular mass complex. *Ub*, ubiquitin.

expression was also weakly detected in adult kidney, where the size of the expressed transcript appeared to be <7 kb. Expression of *NEDL1* in specific regions of the nervous system was further confirmed in the cerebral cortex, corpus callosum, cerebral peduncles, and spinal cord by RT-PCR (Fig. 1*C*). Thus, NEDL1 is a novel HECT-type E3 preferentially expressed in neuronal tissues, including the spinal cord. Using a specific anti-NEDL1 polyclonal antibody that we generated, we localized NEDL1 primarily to the cytoplasm in both intact human neuroblastoma CHP134 cells and COS-7 cells transiently expressing NEDL1 (Fig. 1*D*). The *in vitro* system containing UbcH5c or UbcH7 demonstrated that NEDL1 has a ubiquitin-protein ligase activity (Fig. 1*E*).

NEDL1 Physically Interacts with TRAP-δ and Mutant SOD1—We then sought protein-binding partners of NEDL1 by yeast two-hybrid screening using the region including two WW protein interaction domains (amino acids 757–1114) as bait. Of 96 positive clones subjected to DNA sequencing, one was a full-length cDNA for TRAP-δ; this was of considerable interest, as TRAP-δ was previously reported to bind mutant (G85R and G93A), but not wild-type, SOD1 (9). TRAP-δ is a protein component of the translocon in the ER membrane (10). We therefore examined the interaction among NEDL1, TRAP-δ, and SOD1 by an immunoprecipitation assay after cotransfecting the corresponding expression constructs into COS-7 cells. As shown in Fig. 2 (*A* and *B*), NEDL1 was physically associated with both exogenous and endogenous TRAP-δ probably through the region of two WW domains, as originally suggested by the result of two-hybrid screening. Surprisingly, NEDL1 bound to mutant (but not wild-type) SOD1 (Fig. 2*C*). Furthermore, the degree of binding between NEDL1 and different mutant SOD1 proteins was roughly proportionate to the rapidity of progression (time from clinical onset to death) of the associated FALS phenotype (17–23). For example, two mutant SOD1 proteins associated with an extremely rapid clinical course (C6F and A4V) interacted very strongly with NEDL1. By contrast, the binding of NEDL1 to other mutants was less striking and decreased proportionately to the falloff of disease severity corresponding to those mutants. Of further interest, like the NEDL1-mutant SOD1 interaction, the binding intensity between TRAP-δ and mutant SOD1 was also dependent on the disease severity (Fig. 2*D*). These observations suggest that NEDL1 and TRAP-δ are normally associated with each other, but that misfolded mutant SOD1 makes a complex with them. Such a complex is not formed with wild-type SOD1. The experiments using the *in vitro* translated proteins suggested that association of mutant SOD1 and TRAP-δ was direct (data not shown). It therefore appears that mutant SOD1 forms tightly bound protein complexes with NEDL1 and TRAP-δ and that the tightness of binding in the complex is determined in part by

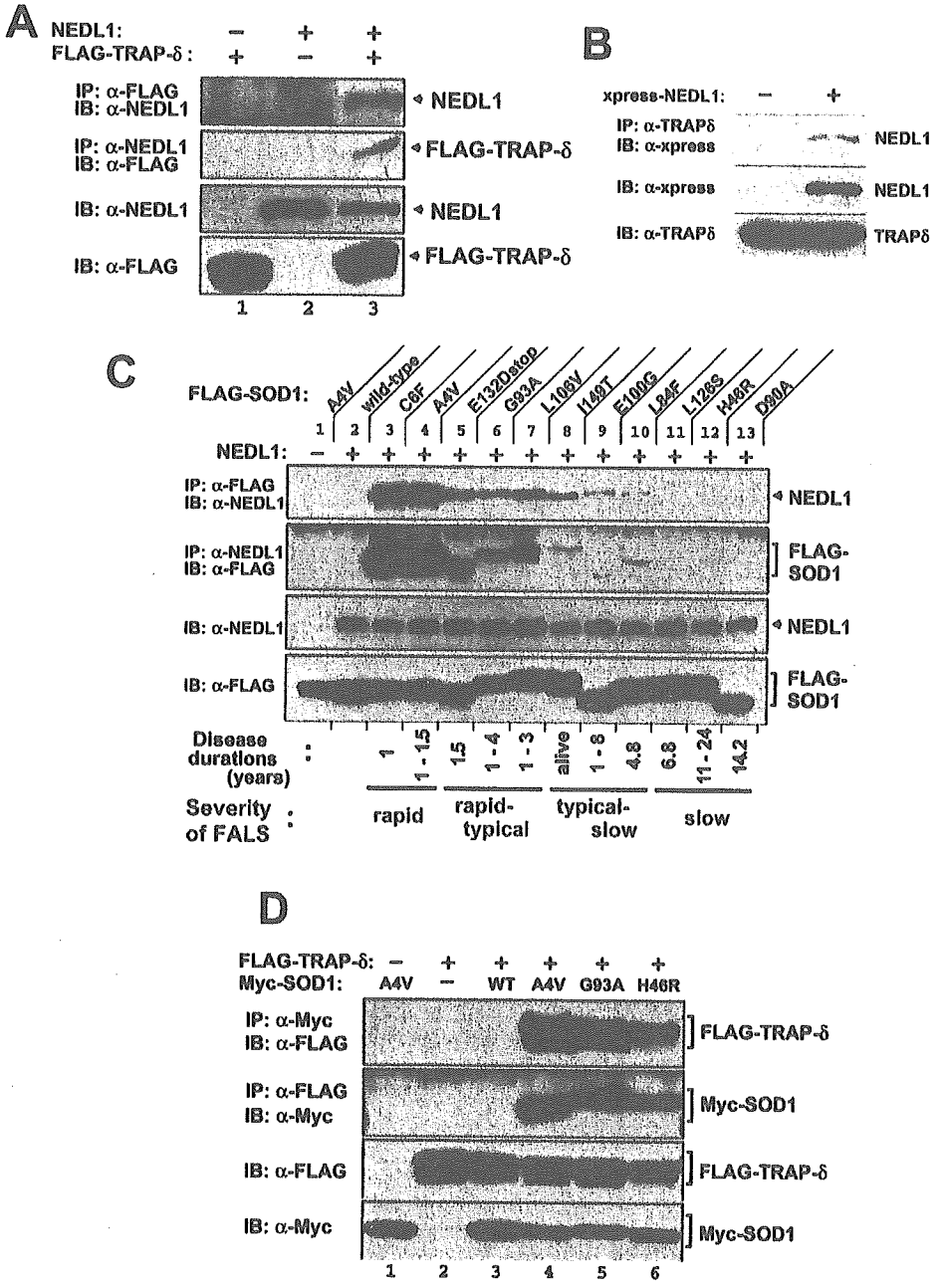

FIG. 2. **NEDL1 interacts with TRAP-δ and FALS-associated mutant forms of SOD1, but not with wild-type SOD1.** *A*, NEDL1 interacts with TRAP-δ. COS-7 cells were cotransfected with the indicated expression plasmids, and whole cell lysates were immunoprecipitated (*IP*) with anti-FLAG (*first panel*) or anti-NEDL1 (*second panel*) antibody. Immunoprecipitates were analyzed by immunoblotting (*IB*) using the indicated antibodies. Whole cell lysates were analyzed for expression levels of each protein by immunoblot analysis (*third* and *fourth panels*). Detection was performed with horseradish peroxidase-conjugated secondary antibodies. *B*, NEDL1 also binds to endogenous TRAP-δ. *C*, interaction between NEDL1 and mutant SOD1. Whole cell lysates from COS-7 cells overexpressing NEDL1 and one of the FLAG-tagged SOD1 mutants or wild-type SOD1 were immunoprecipitated with anti-FLAG (*first panel*) or anti-NEDL1 (*second panel*) antibody and then immunoblotted with anti-NEDL1 or anti-FLAG antibody, respectively. The expression of NEDL1 or FLAG-tagged SOD1 mutants was analyzed by immunoblotting using anti-NEDL1 (*third panel*) or anti-FLAG (*fourth panel*) antibody, respectively. Patients carrying the SOD1(C6F) and SOD1(A4V) mutations have a rapid clinical course, whereas mutant SOD1(L126S), SOD1(H46R), or SOD1(D90A) is associated with a slow clinical course. *D*, interaction of TRAP-δ with mutant SOD1. COS-7 cells were transiently cotransfected with the expression plasmid for FLAG-tagged TRAP-δ and the expression plasmid encoding one of the Myc-tagged SOD1 mutants or wild-type (*WT*) SOD1. Whole cell lysates were immunoprecipitated with anti-Myc (*first panel*) or anti-FLAG (*second panel*) antibody, followed by immunoblotting with anti-FLAG or anti-Myc antibody, respectively. The levels of overexpression of FLAG-tagged TRAP-δ (*third panel*) and Myc-tagged SOD1 (*fourth panel*) were analyzed by immunoblotting using anti-FLAG and anti-Myc antibodies, respectively.

properties of the mutant enzyme that also modulate disease severity of the resulting ALS phenotype. Such complexes do not form in cells with wild-type SOD1.

Determination of the Interaction Domains—We next examined the domains of NEDL1 required for formation of the SOD1·NEDL1·TRAP-δ complex. We generated various constructs of NEDL1 with deletions of each domain. Fig. 3 shows the results of immunoprecipitation assay for the association between deletion mutants of NEDL1 and mutant SOD1(G93A). Mutant SOD1 bound weakly to NEDL1 lacking WW domain-1 (Fig. 3*A*), suggesting that WW domain-1 and its surrounding portion are the region involved in their interaction. Immuno-

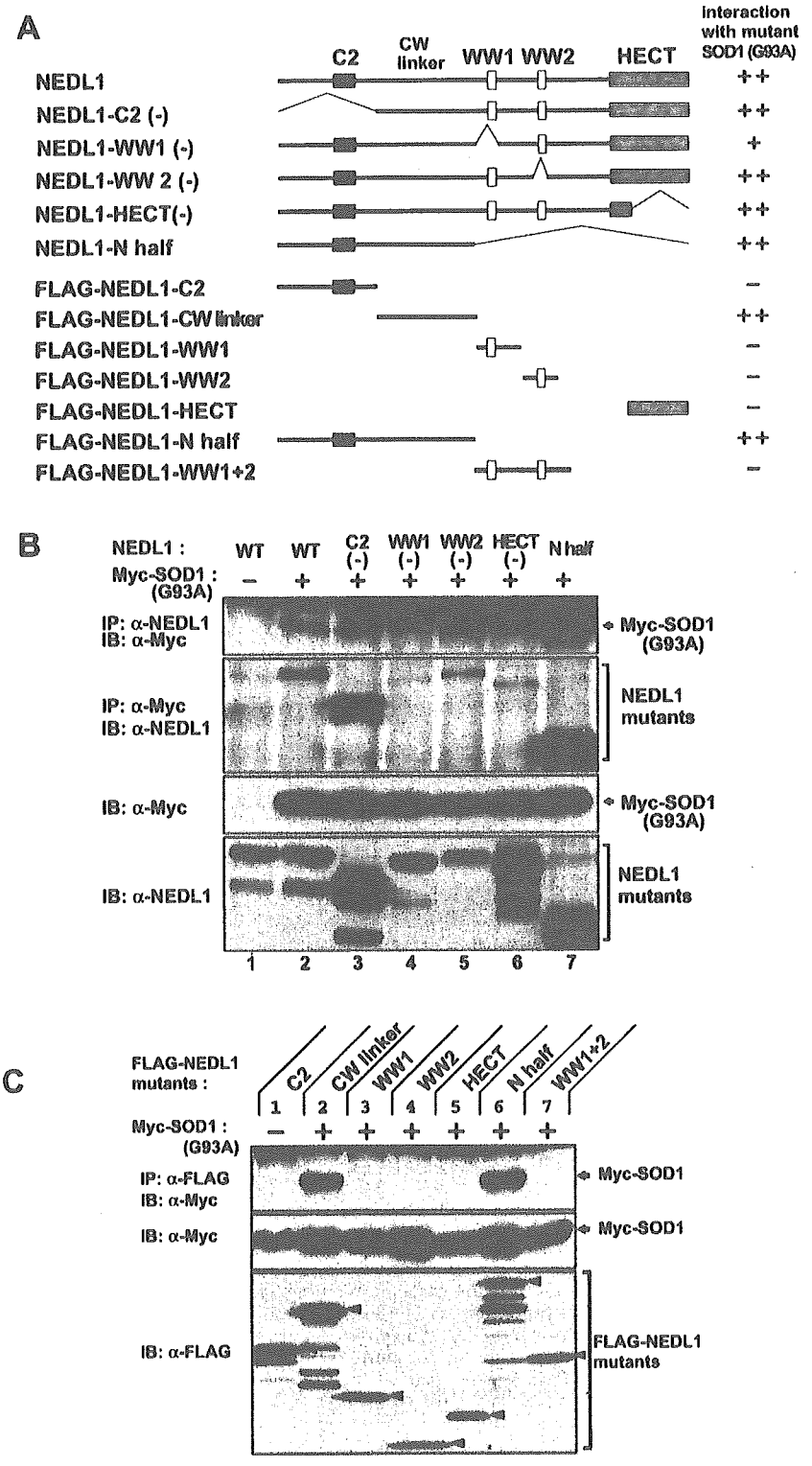

FIG. 3. **The region of NEDL1 between the C2 domain and WW domain-1 is required for interaction with mutant SOD1.** *A*, schematic illustration of wild-type NEDL1 and a series of deletion mutants of NEDL1. *CW linker* indicates the region between the C2 domain and WW domain-1 (*WW1*). *B* and *C*, immunoprecipitation and immunoblot analyses. In *B*, Myc-tagged mutant SOD1(G93A) was overexpressed together with wild-type (*WT*) NEDL1 or the indicated deletion mutants of NEDL1 in COS-7 cells. Whole cell lysates were immunoprecipitated (*IP*) with anti-NEDL1 (*first panel*) or anti-Myc (*second panel*) antibody, followed by immunoblotting (*IB*) with anti-Myc or anti-NEDL1 antibody, respectively. The expression levels of each protein were analyzed by immunoblotting using the indicated antibodies (*third* and *fourth panels*). In *C*, whole cell lysates were immunoprecipitated with anti-FLAG antibody and then immunoblotted with anti-Myc antibody (*upper panel*). Whole lysates were also analyzed by Western blotting for each protein (*middle* and *lower panels*).

precipitation analysis using the specific regions of NEDL1 clearly showed that the region between the C2 domain and WW domain-1 (CW linker region) is necessary for binding to mutant SOD1(G93A). Mutant SOD1(A4V) was also associated with NEDL1 through the same region, and TRAP-δ bound to the two WW domains of NEDL1 (data not shown).

NEDL1 Ubiquitinates Mutant SOD1 for Degradation Depending on the Disease Severity of FALS—Because NEDL1 is an E3, we next tested whether it ubiquitinates TRAP-δ and mutant SOD1 for degradation. As shown in Fig. 4*A*, NEDL1 clearly ubiquitinated mutant SOD1(A4V), but not TRAP-δ (data not shown). Furthermore, the degree of ubiquitination of mutant SOD1 by NEDL1 was dependent on the disease severity of FALS (A4V > G93A > H46R) (Fig. 4*A*). Fig. 4*B* shows the time course of degradation of wild-type and mutant SOD1 in the presence or absence of NEDL1. As reported previously (46), mutant SOD1 was degraded more rapidly than wild-type SOD1. NEDL1 did not affect wild-type SOD1 degradation. As expected from the co-immunoprecipitation and ubiquitination analyses, degradation of mutant SOD1 was stimulated by NEDL1 proportionately to the disease severity of FALS caused by the particular SOD1 mutant (A4V > G93A > H46R ≥

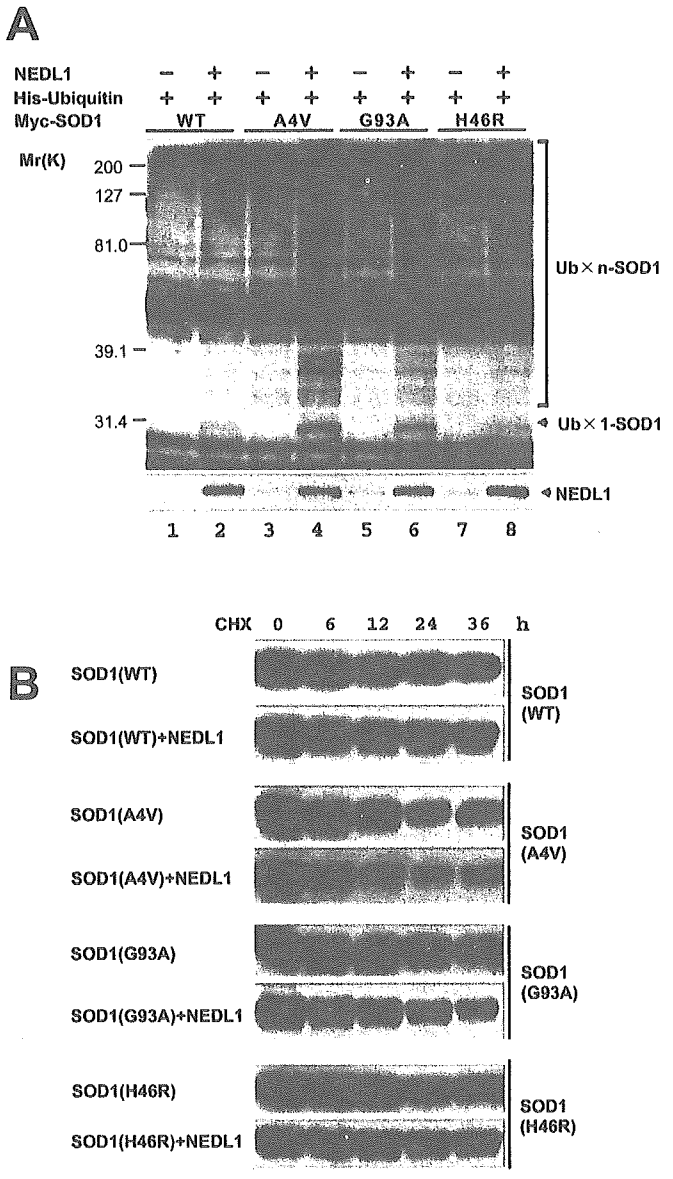

FIG. 4. **NEDL1-dependent ubiquitination and degradation of mutant forms of SOD1 correlate broadly with their respective clinical phenotypes.** *A*, NEDL1 ubiquitinates mutant SOD1 in a mutant type-dependent manner. COS-7 cells were transiently cotransfected with the indicated expression plasmids. Whole cell lysates from transfected COS-7 cells were immunoprecipitated with anti-Myc antibody, and immunoprecipitates were analyzed by Western blotting with anti-ubiquitin (*Ub*) antibody (*upper panel*). The *bracket* indicates slowly migrating ubiquitinated forms of SOD1. Whole cell lysates were analyzed by immunoblotting with anti-NEDL1 antibody to confirm the expression of transfected NEDL1 (*lower panel*). The running positions of molecular weight markers are indicated on the left. *B*, half-lives of wild-type (*WT*) and mutant SOD1 proteins in the presence or absence of NEDL1. Cell lysates were harvested from Neuro2a cells transfected with *SOD1* alone or with *SOD1* plus *NEDL1* at different time points as indicated after the addition of cycloheximide (*CHX*; final concentration of 50 μg/ml) and were analyzed for SOD1 protein levels by Western blotting with anti-FLAG antibody. In the presence of NEDL1, the half-lives of various mutant SOD1 proteins were reduced also roughly dependent on the disease severity of FALS (A4V > G93A > H46R).

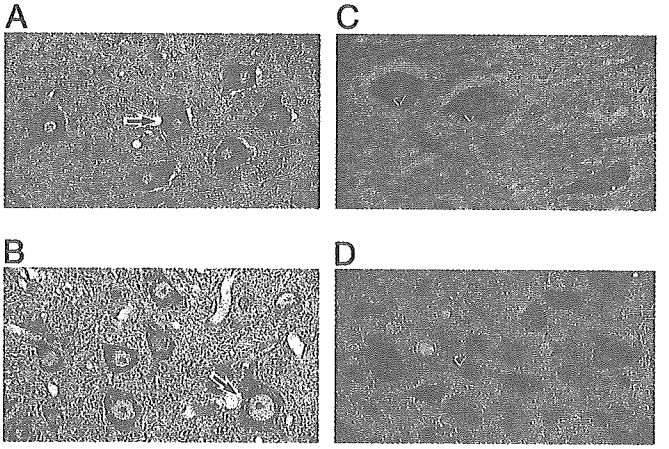

FIG. 5. **NEDL1 immunohistochemical analyses.** *A*, immunohistochemical analysis of NEDL1 in normal human spinal cord. NEDL1-positive anterior horn cells are evident (*arrow*), although the immunoreactivity for NEDL1 is somewhat faint. There was no counterstaining. Magnification ×520. *B*, NEDL1 immunohistochemistry in normal mouse spinal cord. Normal anterior horn cells are positive for NEDL1 (*arrow*). The section was counterstained with hematoxylin. Magnification ×750. *C*, immunostaining for NEDL1 in spinal cord LBHIs from an FALS patient with a frameshift 126 mutation in the *SOD1* gene. The NEDL1-positive reaction products were mostly restricted to the cores of the core and halo-type LBHIs (*arrowheads*). In the LBHI-bearing neurons and residual neurons, the antibody to NEDL1 also stained the neuronal cell body. There was no counterstaining. Magnification ×540. *D*, NEDL1 immunostaining in a spinal cord LBHI from an *SOD1*(H46R) transgenic mouse. An ill defined LBHI in the *SOD1*(H46R) transgenic mouse was positive for NEDL1; this ill defined LBHI shows a diffuse staining pattern (*arrowhead*). The staining intensity in the residual neurons stained by anti-NEDL1 antibody varied from neuron to neuron. The section was counterstained with hematoxylin. Magnification ×770.

wild-type). Thus, NEDL1 targeted mutant SOD1 for ubiquitin-mediated degradation in the cell in parallel with the binding intensity.

Immunohistochemistry—One of the characteristic cytopathological changes of mutant SOD1-linked FALS is the formation of neuronal Lewy body-like hyaline inclusions (LBHIs) that contain aggregates of SOD1 and ubiquitin (24). We therefore performed immunostaining to determine whether the NEDL1 protein is included within the LBHIs of the spinal cord motor neurons obtained from two siblings with FALS caused by frameshift 126 mutation of SOD1 (11, 12). One case had neuropathological findings compatible with FALS with posterior column involvement, whereas the other had multisystem degeneration in addition to motor neuron disturbance. We also performed NEDL1 immunostaining in specimens obtained from mutant *SOD1*(H46R) transgenic mice at 180 days, by which time they show clinical motor signs in the hind limbs (13). The specificity of the NEDL1 staining was confirmed by pretreating the specimens with an excess of NEDL1 antigen. NEDL1 immunoreactivity in the spinal cords of the human control cases was identical to that of normal mice: immunoreactivity was identified predominantly in the cytoplasm of the neurons of the spinal cords (Fig. 5, *A* and *B*). The LBHIs in the anterior horn cells of two FALS patients and transgenic mice showed equivalent immunoreactivity for NEDL1. Although the intensity of NEDL1 immunoreactivity in neuronal LBHIs varied, most of the LBHIs were immunoreactive for NEDL1 (Fig. 5, *C* and *D*). The reaction products were generally restricted to the cores of the core and halo-type LBHIs that showed eosinophilic cores with pale peripheral halos upon hematoxylin and eosin staining (Fig. 5*C*); by contrast, immunopositive NEDL1 in ill defined LBHIs was distributed throughout the inclusions (Fig. 5*D*). NEDL1 immunoreactivity in the residual neurons in humans and mice was identified primarily in cell bodies. Thus, NEDL1 immunostaining was clearly positive in the FALS-related LBHIs that were also positive for ubiquitin and SOD1 (data not shown).

NEDL1 Targets Dishevelled-1 for Ubiquitin-mediated Protein Degradation—We next hypothesized that the physiological function of NEDL1 to mediate ubiquitination is interfered with

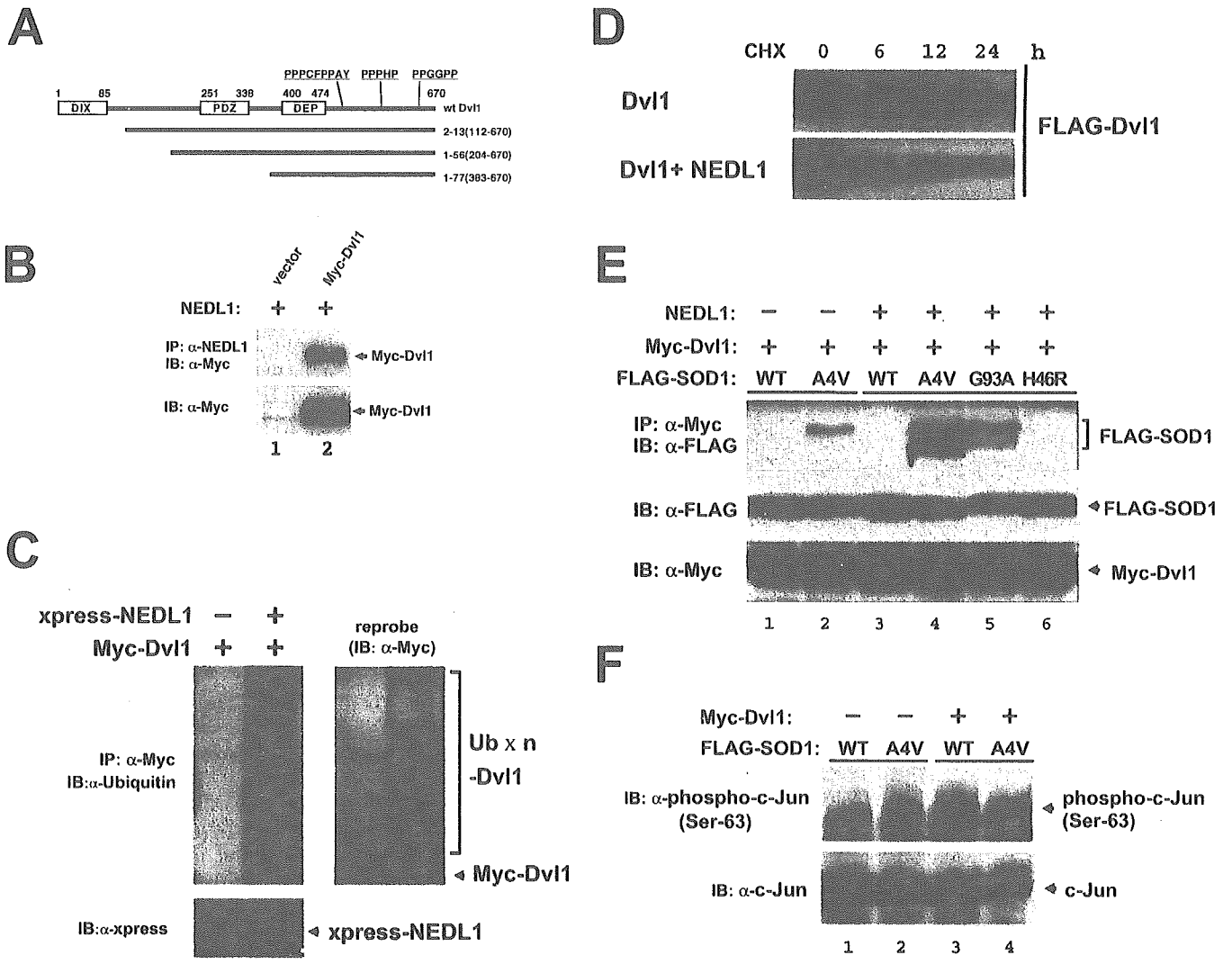

FIG. 6. **Dvl1 is a substrate of NEDL1, and its functions are disturbed by mutant SOD1(A4V).** *A*, schematic illustration of full-length Dvl1 and three clones obtained by yeast two-hybrid screening. Human Dvl1 consists of 670 amino acids and contains three conserved domains, including the DIX, PDZ, and DEP domains. Between the DEP domain and the C-terminal end, there are three proline-rich clusters, which might act as WW domain recognition sites. All three clones (clones 2–13, 1–56, 1–77) contain the DEP domain and these clusters. *B*, NEDL1 interacts with Dvl1. Myc-tagged Dvl1 was overexpressed together with NEDL1 in Neuro2a cells. Whole cell lysates were immunoprecipitated (*IP*) with anti-NEDL1 antibody, followed by immunoblotting (*IB*) with anti-Myc antibody (*upper panel*). The expression levels of Myc-tagged Dvl1 were analyzed by immunoblotting using anti-Myc antibody (*lower panel*). *C*, NEDL1 ubiquitinates Dvl1 in Neuro2a cells. The cells were transiently transfected with the indicated expression plasmids along with the ubiquitin expression plasmid in the presence or absence of the expression plasmid for XPRESS-tagged NEDL1. Whole cell lysates were immunoprecipitated with anti-Myc antibody and then immunoblotted with anti-ubiquitin antibody (*left panel*). The ladder of bands denoted by the *bracket* appeared to be ubiquitinated Dvl1. The expression of XPRESS-NEDL1 was analyzed by immunoblotting using anti-XPRESS antibody. The membrane was reprobed with anti-Myc antibody (*right panel*). *D*, Dvl1 is degraded by NEDL1. Neuro2a cells were transfected with the expression plasmid for FLAG-tagged Dvl1 with or without the NEDL1 expression plasmid. Transfected cells were harvested at different time points as indicated after the addition of cycloheximide (*CHX*; final concentration of 50 μg/ml), and Dvl1 protein levels were analyzed by Western blotting with anti-FLAG antibody. In the presence of NEDL1, the half-lives of FLAG-Dvl1 were significantly reduced. *E*, Dvl1 binds to mutant SOD1(A4V), and the degree of its binding is enhanced in the presence of NEDL1. Whole cell lysates prepared from COS-7 cells transfected with the indicated combinations of expression plasmids were subjected to immunoprecipitation and Western analyses as indicated. *F*, c-Jun phosphorylation by overexpression of Dvl1 is suppressed upon coexpression of mutant SOD1(A4V). Whole cell lysates from COS-7 cells transfected with the indicated combinations of expression plasmids were subjected to Western blotting with antibody against the phosphorylated form of c-Jun (*upper panel*) or with anti-c-Jun antibody (*lower panel*). *wt/WT*, wild-type.

by mutant SOD1. To test this hypothesis, we again performed yeast two-hybrid screening to obtain NEDL1-interacting molecules using the large region of NEDL1 (amino acids 382–1448) as bait. Of 396 His and β-galactosidase double-positive clones, 282 clones were subjected to DNA sequencing, and we identified Dvl1 (three clones). Human Dvl1 is a 670-amino acid protein with three conserved domains: a DIX domain, which is required for canonical Wnt/T-cell factor signaling; a PDZ domain, which is a target of both Stbm and casein kinase I binding; and a DEP domain, which is responsible for Dvl membrane localization during planar cell polarity signaling (25–27). Between the DEP domain and C-terminal end, there are three proline-rich clusters unique to mammalian Dvl1, which presumably act as the WW domain recognition sites. All three clones (clones 2–13, 1–56, and 1–77) contain the DEP domain and proline-rich clusters, suggesting that NEDL1 interacted with Dvl1 in the C-terminal half (Fig. 6*A*). In Neuro2a cells, NEDL1 co-immunoprecipitated with Dvl1 (Fig. 6*B*) and ubiquitinated it for degradation (Fig. 6, *C* and *D*). Thus, Dvl1 may be one of the physiological targets of NEDL1 E3. As recent studies strongly suggest that the cytotoxicity of SOD1 mutants is responsible for their aggregate properties, incorporating other proteins essential for cells into their aggregates (28), we examined the association between mutant SOD1 and Dvl1,

both of which interact with NEDL1. Of interest, Dvl1 bound to mutant SOD1(A4V), and complex formation was increased in the presence of NEDL1 roughly proportionately to the disease severity of FALS caused by the particular SOD1 mutant (Fig. 6*E*). Dvl1 is known to transduce not only the Wnt/β-catenin/T-cell factor pathway, but also the JNK/c-Jun pathway (27). Therefore, we next examined whether the Dvl1-induced phosphorylation of c-Jun at Ser^{63} was affected by the tight complex formation induced by inclusion of mutant SOD1. As shown in Fig. 6*F*, c-Jun phosphorylation induced by overexpression of Dvl1 was significantly suppressed by coexpression with mutant SOD1(A4V) in COS-7 cells.

DISCUSSION

Our present results demonstrate that a novel HECT-type NEDL1 E3, which is preferentially expressed in neuronal tissues, specifically targets mutant forms of SOD1 for ubiquitination-mediated protein degradation. NEDL1 is also associated with TRAP-δ localized at the ER translocon. The TRAP complex has recently been shown to facilitate the initiation of protein translocation in a substrate-specific manner (29). The NEDL1·TRAP-δ complex recognizes mutant (but not wild-type) SOD1, with a binding intensity that broadly parallels the disease severity of FALS. NEDL1 immunoreactivity was detected in the FALS-related LBHIs in the spinal cord ventral horn motor neurons, suggesting that, although mutant SOD1 is ubiquitinated for degradation by NEDL1, the mutant SOD1·NEDL1·TRAP-δ complex aggregates within the LBHIs. It is also conceivable that fragmentation of the Golgi apparatus reported in ALS patients and transgenic mice might be related to this aggregation (30, 31). These findings suggest possible hypotheses for the role of NEDL1 in the pathogenesis of FALS: 1) NEDL1, alone or with TRAP-δ, ubiquitinates and aggregates mutant SOD1, thereby decreasing the function of mutant SOD1; 2) NEDL1 and TRAP-δ form aggregates with mutant SOD1 that induce fragmentation of the Golgi apparatus, leading to neuronal apoptosis; 3) formation of these aggregates causes dysfunction of NEDL1 and/or TRAP-δ, and this, in turn, induces disturbances that ultimately cause motor neuron death; and 4) the mutant SOD1·NEDL1·TRAP-δ aggregates trap and inactivate unknown factor(s) such as molecular chaperones whose normal function is important for motor neuron viability.

To further understand the role of NEDL1 in motor neuron death, we searched for the physiological targets of NEDL1 and identified Dvl1. As expected, Dvl1 is ubiquitinated for degradation by NEDL1. Surprisingly, however, Dvl1 also interacts with mutant SOD1 in the presence of NEDL1 roughly proportionately to the disease severity of FALS caused by the particular SOD1 mutant. Dvl1, an essential multimodule signal transducer localized in the cellular cytosol and cytoskeleton, mediates planar cell polarity signaling as well as canonical Wnt/β-catenin signaling (27, 32). In mammals, three Dvl family members have so far been reported, and the level of Dvl1 expression is high in neuronal tissues (33). As far as we know, NEDL1 is the first E3 for Dvl1, interacting with the C-terminal region containing three proline-rich clusters. A recent report suggests that Dvl1 regulates microtubule stability through inhibition of glycogen synthase kinase-3β (34). Because cytoskeletal abnormalities have been reported in ALS motor neurons (35), it is possible that the effect of mutant SOD1 on NEDL1-mediated Dvl1 degradation is involved in the motor neuron death. Furthermore, Dvl1 is abundant in the postsynaptic membrane region at the neuromuscular junction (36) that is reported to be involved in several neurodegenerative disorders (37, 38). Of interest, *Dvl1* is mapped to chromosome 1p36, which is a commonly deleted region in many human cancers, including neuroblastoma (39). As NEDL1 is highly expressed in neuroblastomas with favorable prognosis, which have a tendency to differentiate and/or regress, NEDL1 may be involved in the regulation of neuronal differentiation and survival possibly by controlling Dvl1.

NEDL1, TRAP-δ, mutant SOD1, and Dvl1 appear to form a complex roughly proportionately to the disease severity of FALS caused by the particular SOD1 mutant. Our present observations strongly suggest that NEDL1 may be a quality control E3 recognizing misfolded mutant SOD1 (40). The association between mutant SOD1 and NEDL1 may induce the conformational change in the NEDL1 protein to increase the binding intensity with other physiological targets such as TRAP-δ (not ubiquitinated) and Dvl1 (ubiquitinated). This may lead to tight complex formation especially when the proteasome activity is impaired. It has been reported that the expression and function of proteasomes decrease with age in the spinal cord (7). Okado-Matsumoto and Fridovich (41) have also found that complex formation between mutant SOD1 and heat shock proteins leads to protein aggregates. Because our data show that the ER translocon component TRAP-δ is involved, aggregate formation may occur at the sites of the ER or Golgi apparatus or even at other cellular sites. The complex formation including NEDL1 and mutant SOD1 may conversely affect the physiological function of NEDL1, as demonstrated by a decrease in Dvl1-induced phosphorylation of c-Jun.

Recently, the RING finger-type E3 Dorfin has been reported to ubiquitinate mutant SOD1 for degradation (42). However, NEDL1 and Dorfin appear to be different in several aspects. First, NEDL1 is expressed specifically in neuronal tissues, including the spinal cord, whereas Dorfin is ubiquitously expressed in most human tissues. Second, both interaction between NEDL1 and mutant SOD1 and ubiquitination of the latter by NEDL1 roughly parallel the disease severity caused by the particular SOD1 mutant, whereas Dorfin similarly ubiquitinates mutant forms of SOD1. In addition, we have identified Dvl1 and TRAP-δ as cellular target proteins of NEDL1, whereas the physiological targets of Dorfin have never been reported. It is probable that there are some other E3 ligases targeting mutant SOD1. However, the molecular characteristics, including tissue-specific expression, subcellular localization, and age-dependent expression, might be important in the development of the FALS phenotype.

In conclusion, we have identified a novel neuronal E3 (NEDL1) that interacts with TRAP-δ and also binds to and ubiquitinates Dvl1 for degradation. Strikingly, NEDL1 targets and ubiquitinates mutant (but not wild-type) SOD1 for degradation. NEDL1 may normally function in the quality control of cellular proteins by eliminating misfolded proteins such as mutant SOD1, possibly via a mechanism analogous to that of ER-associated degradation (43–45). NEDL1 appears to complex tightly with mutant SOD1, Dvl1, and TRAP-δ, forming aggregates with species of mutant SOD1 that have escaped ubiquitin-mediated degradation. The NEDL1 function that affects the activities of the target proteins may also be modulated by mutant SOD1. All of these might contribute to the pathogenesis of FALS; further elucidation of the molecular mechanism of formation of this complex and its pathogenicity may provide insights into motor neuron death in ALS as well as possible new therapeutic strategies for ALS.

Acknowledgments—We thank Robert H. Brown, Jr. (Harvard Medical School) for critical comments and reading the manuscript. We also thank M. Ohira and Y. Nakamura for helping with cDNA cloning and sequencing; K. Watanabe and M. Suzuki for making plasmid constructs; M. Nagai and M. Kato for helping with immunohistochemical studies; S. Hatakeyama, M. Matsumoto, and K. Nakayama

for ubiquitination assay instruction; and S. Sakiyama for reading the manuscript.

REFERENCES

1. Rosen, D. R., Siddique, T., Patterson, D., Figlewicz, D. A., Sapp, P., Hentati, A., Donaldson, D., Goto, J., O'Regan, J. P., Deng, H. X., Rahmani, Z., Krizus, A., McKenna-Yasek, D., Cayabyab, A., Gaston, S. M., Berger, R., Tanzi, R. E., Halperin, J. J., Herzfeldt, B., van den Bergh, R., Hung, W.-Y., Bird, T., Deng, G., Mulder, D. W., Smyth, C., Laing, N. G., Soriano, E., Pericak-Vance, M. A., Haines, J., Rouleau, G. A., Gusella, J. S., Horvitz, H. R., and Brown, R. H., Jr. (1993) *Nature* **364,** 59–62
2. Deng, H. X., Hentati, A., Tainer, J. A., Iqbal, Z., Cayabyab, A., Hung, W.-Y., Getzoff, E. D., Hu, P., Herzfeldt, B., Roos, R. P., Warner, C., Deng, G., Soriano, E., Smyth, C., Parge, H. E., Ahmed, A., Roses, A. D., Hallewell, R., Rericak-Vance, M. A., and Siddique, T. (1993) *Science* **261,** 1047–1051
3. Cleveland, D. W., and Liu, J. (2001) *Nat. Med.* **6,** 1320–1321
4. Brown, R. H., Jr., and Robberecht, W. (2001) *Semin. Neurol.* **21,** 131–139
5. Cluskey, S., and Ramsden, D. B. (2001) *Mol. Pathol.* **54,** 386–392
6. Orrell, R. W., and Figlewicz, D. A. (2001) *Neurology* **57,** 9–17
7. Keller, J. N., Huang, F. F., and Markesbery, W. R. (2000) *Neuroscience* **98,** 149–156
8. Hoffman, E. K., Wilcox, H. M., Scott, R. W., and Siman, R. (1996) *J. Neurol. Sci.* **139,** 15–20
9. Kunst, C. B., Mezey, E., Brownstein, M. J., and Patterson, D. (1997) *Nat. Genet.* **15,** 91–94
10. Hartmann, E., Gorlich, D., Kostka, S., Otto, A., Kraft, R., Knespel, S., Burger, E., Rapoport, T. A., and Prehn, S. (1993) *Eur. J. Biochem.* **214,** 375–381
11. Kato, S., Shimoda, M., Watanabe, Y., Nakashima, K., Takahashi, K., and Ohama, E. (1996) *J. Neuropathol. Exp. Neurol.* **55,** 1089–1101
12. Kato, S., Hayashi, H., Nakashima, K., Nanba, E., Kato, M., Hirano, A., Nakano, I., Asayama, K., and Ohama, E. (1997) *Am. J. Pathol.* **151,** 611–620
13. Nagai, M., Aoki, M., Miyoshi, I., Kato, M., Pasinelli, P., Kasai, N., Brown, R. H., Jr., and Itoyama, Y. (2001) *J. Neurosci.* **21,** 9246–9254
14. Nakagawara, A. (1998) *Med. Pediatr. Oncol.* **31,** 113–115
15. Harvey, K. F., and Kumar, S. (1999) *Trends Cell Biol.* **9,** 166–169
16. Kumar, S., Tomooka, Y., and Noda, M. (1992) *Biochem. Biophys. Res. Commun.* **30,** 1155–1161
17. Kato, S., Takikawa, M., Nakashima, K., Hirano, A., Cleveland, D. W., Kusaka, H., Shibata, N., Kato, M., Nakano, I., and Ohama, E. (2000) *Amyotroph. Lateral Scler. Other Motor Neuron Disord.* **1,** 163–184
18. Orrell, R. W. (2000) *Neuromuscul. Disord.* **10,** 63–68
19. Cudkowicz, M. E., McKenna-Yasek, D., Sapp, P. E., Chin, W., Geller, B., Hayden, D. L., Schoenfeld, D. A., Hosler, B. A., Horvitz, H. R., and Brown, R. H., Jr. (1997) *Ann. Neurol.* **41,** 210–221
20. Ratovitski, T., Corson, L. B., Strain, J., Wong, P., Cleveland, D. W., Culotta, V. C., and Borchelt, D. R. (1999) *Hum. Mol. Genet.* **8,** 1451–1460
21. Aoki, M., Ogasawara, M., Matsubara, Y., Narisawa, K., Nakamura, S., Itoyama, Y., and Abe, K. (1993) *Nat. Genet.* **5,** 323–324
22. Kato, M., Aoki, M., Ohta, M., Nagai, M., Ishizaki, F., Nakamura, S., and Itoyama, Y. (2001) *Neurosci. Lett.* **312,** 165–168
23. Andersen, P. M., Forsgren, L., Binzer, M., Nilsson, P., Ala-Hurula, V., Keranen, M. L., Bergmark, L., Saarinen, A., Haltia, T., Tarvainen, I., Kinnunen, E., Udd, B., and Marklund, S. L. (1996) *Brain* **119,** 1153–1172
24. Shibata, N., Hirano, A., Kobayashi, M., Siddique, T., Deng, H. X., Hung, W.-Y., Kato, T., and Asayama, K. (1996) *J. Neuropathol. Exp. Neurol.* **55,** 481–490
25. Sussman, D. J., Klingensmith, J., Salinas, P., Adams, P. S., Nusse, R., and Perrimon, N. (1994) *Dev. Biol.* **166,** 73–86
26. Wodarz, A., and Nusse, R. (1998) *Annu. Rev. Cell Dev. Biol.* **14,** 59–88
27. Boutros, M., Paricio, N., Strutt, D. I., and Mlodzik, M. (1998) *Cell* **94,** 109–118
28. Julien, J. P. (2001) *Cell* **104,** 581–591
29. Fons, R. D., Bogert, B. A., and Hegde, R. S. (2003) *J. Cell Biol.* **160,** 529–539
30. Fujita, Y., Okamoto, K., Sakurai, A., Gonatas, N. K., and Hirano, A. (2000) *J. Neurol. Sci.* **174,** 137–140
31. Mourelatos, Z., Gonatas, N. K., Stieber, A., Gurney, M. E., and Dal Canto, M. C. (1996) *Proc. Natl. Acad. Sci. U. S. A.* **93,** 5472–5477
32. Wharton, K. A., Jr. (2003) *Dev. Biol.* **253,** 1–17
33. Tsang, M., Lijam, N., Yang, Y., Beier, D. R., Wynshaw-Boris, A., and Sussman, D. J. (1996) *Dev. Dyn.* **207,** 253–262
34. Krylova, O., Messenger, M. J., and Salinas, P. C. (2000) *J. Cell Biol.* **151,** 83–94
35. Julien, J. P., and Beaulieu, J. M. (2000) *J. Neurol. Sci.* **180,** 7–14
36. Luo, Z. G., Wang, Q., Zhou, J. Z., Wang, J., Luo, Z., Liu, M., He, X., Wynshaw-Boris, A., Xiong, W. C., Lu, B., and Mei, L. (2002) *Neuron* **35,** 489–505
37. De Ferrari, G. V., and Inestrosa, N. C. (2000) *Brain Res. Brain Res. Rev.* **33,** 1–12
38. Kaytor, M. D., and Orr, H. T. (2000) *Curr. Opin. Neurobiol.* **12,** 275–278
39. Versteeg, R., Caron, H., Cheng, N. C., van der Drift, P., Slater, R., Westerveld, A., Voute, P. A., Delattre, O., Laureys, G., van Roy, N., and Speleman, F. (1995) *Eur. J. Cancer* **31,** 538–541
40. Murata, S., Minami, Y., Minami, M., Chiba, T., and Tanaka, K. (2001) *EMBO Rep.* **2,** 1133–1138
41. Okado-Matsumoto, A., and Fridovich, I. (2002) *Proc. Natl. Acad. Sci. U. S. A.* **99,** 9010–9014
42. Niwa, J., Ishigaki, S., Hishikawa, N., Yamamoto, M., Doyu, M., Murata, S., Tanaka, K., Taniguchi, N., and Sobue, G. (2002) *J. Biol. Chem.* **277,** 36793–36798
43. Mori, K. (2000) *Cell* **101,** 451–454
44. Travers, K. J., Patil, C. K., Wodicka, L., Lockhart, D. J., Weissman, J. S., and Walter, P. (2000) *Cell* **101,** 249–258
45. Wickner, S., Maurizi, M. R., and Gottesman, S. (1999) *Science* **286,** 1888–1893
46. Borchelt, D. R., Lee, M. K., Slunt, H. S., Guarnieri, M., Xu, Z. S., Wong, P. C., Brown, R. H., Jr., Price, D. L., Sisodia, S. S., and Cleveland, D. W. (1994) *Proc. Natl. Acad. Sci. U. S. A.* **16,** 8292–8296

Identification of novel human neuronal leucine-rich repeat (h*NLRR*) family genes and inverse association of expression of *Nbla10449*/h*NLRR-1* and *Nbla10677*/h*NLRR-3* with the prognosis of primary neuroblastomas

SHIHO HAMANO[1,2], MIKI OHIRA[1], ERIKO ISOGAI[1], KOUNOSUKE NAKADA[2] and AKIRA NAKAGAWARA[1]

[1]Division of Biochemistry, Chiba Cancer Center Research Institute, 666-2 Nitona, Chuoh-ku, Chiba 260-8717; [2]Division of Pediatric Surgery, St. Marianna University School of Medicine, 2-16-1 Sugao, Miyamae-ku, Kawasaki 216-8511, Japan

Received August 1, 2003; Accepted September 24, 2003

Abstract. To search for novel prognostic indicators, we previously cloned >2,000 novel genes from primary neuroblastoma (NBL) cDNA libraries and screened for differential expression between the subsets with favorable (stage 1 or 2 with a single copy of *MYCN*) and unfavorable (stage 3 or 4 with amplification of *MYCN*) prognosis. From them, we have identified 3 genes of human neuronal leucine-rich repeat protein (NLRR) family: *Nbla10449*/h*NLRR-1*, *Nbla00061*/h*NLRR-2*/*GAC1* and *Nbla10677*/h*NLRR-3*. An additional family member, h*NLRR-5*, was also found by homology search against public database. NLRR family proteins have been proposed to function as a neuronal adhesion molecule or soluble ligand binding receptor like *Drosophila toll* and *slit* with multiple domains including 11 sets of extracellular leucine-rich repeat (LRR)-motifs. However, the functional role of the NLRR protein family has been elusive. Our present study shows that h*NLRR* mRNAs are preferentially expressed in nervous system and/or adrenal gland. In cancer cell lines, h*NLRR-1*, h*NLRR-3* and h*NLRR-5* are expressed at high levels in the neural crest-derived cells. Most remarkably, in primary NBLs, h*NLRR-1* is significantly expressed at high levels in unfavorable subsets as compared to favorable ones, whereas the expression pattern of h*NLRR-3* and h*NLRR-5* is the opposite. In order to understand the function of these receptors, we have used newborn mouse superior cervical ganglion (SCG) cells which are dependent on nerve growth factor (NGF) for their survival. Expression of the mouse counterparts of h*NLRR-2* and h*NLRR-3* is up-regulated after NGF-induced differentiation and down-regulated after NGF depletion-induced apoptosis. On the other hand, expression of h*NLRR-1* and h*NLRR-5* is inversely regulated in the same system. These results have suggested that the regulation of the h*NLRR* family genes may be associated with NGF signaling pathway in both SCG cells and neuroblastoma. Our quantitative real-time RT-PCR analysis using 99 primary NBLs has revealed that high levels of h*NLRR-1* expression are significantly associated with older age (>1 year, p=0.0001), advanced stages (p=0.0007), low expression of *TrkA* (p=0.011), and *MYCN* amplification (p=0.0001), while those of h*NLRR-3* expression are significantly correlated with the favorable prognostic indicators. Furthermore, multivariate analysis reveals that expression of h*NLRR-1* is an independent prognostic indicator in human neuroblastoma. Thus, our results demonstrate that, despite being members of the same family, h*NLRR-1* and h*NLRR-3* may share different biological function among the NBL subsets, and that their expression level becomes novel prognostic indicators of NBL.

Introduction

Neuroblastoma (NBL) is one of the most common pediatric tumors originating from sympathoadrenal lineage of the neural crest. NBL shows variable biological behavior which characterizes different clinical subsets (1). The tumors found in young children, <1 year of age usually regress spontaneously, while those in the older children are often aggressive leading to poor outcome. Recent advances in molecular biology have identified the important molecules involved in the regulation of growth, differentiation and programmed cell death during development of the sympathoadrenal cells (2), some of which link to the modulation of NBL biology. These include Trk family tyrosine kinase receptors and *MYCN* proto-oncogene. TrkA, a high-affinity receptor for nerve growth factor (NGF), is expressed in favorable subsets of NBL and regulates differentiation and/or regression of the tumor cells (3). On the other hand, TrkB, a receptor for brain-derived neurotrophic factor (BDNF) and neurotrophin-4 (NT-4), is expressed in NBLs with unfavorable prognosis. An autocrine loop of BDNF/NT-4 and TrkB may promote tumor cell survival and increase their invasiveness (4). Amplification of *MYCN* is significantly associated with allelic loss of the

Correspondence to: Dr Akira Nakagawara, Division of Biochemistry, Chiba Cancer Center Research Institute, 666-2 Nitona, Chuoh-ku, Chiba 260-8717, Japan
E-mail: akiranak@chiba-ccri.chuo.chiba.jp

Key words: leucine-rich repeat, neuroblastoma, differential expression, prognostic factor

distal region of chromosome 1, and both are indicators of poor prognosis. A recent report suggests that *MYCN* oncoprotein induces expression of *Id-2* with a helix-loop-helix domain and in turn negatively regulates Rb tumor suppressor in NBL (5). However, many important genes may still be missing for better understanding of NBL biology as well as predicting the prognosis. In order to identify novel NBL-related genes and promote better understanding of the molecular mechanism of NBL genesis and its biology, differential screening method has been applied (6).

We have previously constructed full-length-enriched oligocapping cDNA libraries from different subsets of primary NBL (6,7). One derived from the mixture of favorable NBLs in stage 1 with single-copy of *MYCN*, and the other from unfavorable NBLs in stage 3 and 4 with *MYCN* amplification. We have finished end-sequencing of 2,500 clones obtained from each library, and found that the expression profile is markedly different between the subsets. So far, 1,800 independent genes from these libraries have been subjected to semi-quantitative RT-PCR using 16 favorable and 16 unfavorable NBLs to find the genes differentially expressed between favorable (F) and unfavorable (UF) subsets (8,9).

In this study, we have identified novel human *NLRR* family genes that are differentially expressed among the NBL subsets. NLRRs are proteins with leucine-rich repeat (LRR) domains which may be involved in protein-protein interactions (10). They may also function as cell-adhesion molecules or signaling receptors implicated in regulation of the neural development. Expression of the h*NLRR-1/Nbla10449* gene is significantly associated with short survival as well as conventional poor-prognostic factors, whereas that of the h*NLRR-3/Nbla10677* gene is increased in favorable subset of NBL. Our results suggest that the differential expression of h*NLRR* genes among the NBL subsets is involved in the regulation of growth, differentiation and cell death of human NBL.

Materials and methods

Patients. We studied tumors from 99 children with NBL diagnosed between 1995-1999. Fifty-four Japanese patients were identified by a mass screening program started in 1985 (9,10). The selection of tumors for this study was solely based on the availability of a sufficient amount of tumor tissue, from which DNA and mRNA could be prepared for the analyses described below.

The diagnosis of NBL was confirmed by histologic assessment of the tumor specimen obtained at surgery according to the classification of Shimada *et al* (11). There were 57 tumors with favorable histology, and 42 with unfavorable histology. The tumors were staged according to the International Neuroblastoma Staging System (INSS) (12). Thirty-eight tumors (36 identified by mass screening) were stage 1, 14 (11 identified by mass screening) stage 2, 5 (3 identified by mass screening) stage 4s, 10 (3 identified by mass screening) stage 3, and 32 (1 identified by mass screening) stage 4. The patients were treated according to the protocols previously described (13).

Tumor samples and cell lines. Fresh, frozen tumorous tissues were sent to the Division of Biochemistry, Chiba Cancer Center Research Institute, from various hospitals in Japan with informed consent from the patient's parents. All samples were obtained by surgery (or biopsy) and stored at -80°C. Studies were approved by the Institutional Review Board of the Chiba Cancer Center. Human cell lines which we used included NBL (CHP134, CHP901, GANB, GOTO, IMR32, SMS-KAN, SMS-KCN, KP-N-NS, LAN-5, NB-1, NB-9, NBKM-1, NB (Tu)-1, NLF, NMB, RTBM1, SMS-SAN, SK-N-BE, SK-N-DZ, TNB, TGW, LHN, NGP, NB69, NBL-S, OAN, SK-N-AS, SK-N-SH, SH-SY5Y, and CNB-RT), osteosarcoma (OST, Saos2, and NOS1), rhabdomyosarcoma (RMS-MK and ASPS-KY), colorectal adenocarcinoma (COLO320, SW480, and LOVO), a hepatocellular cancer (HepG2), breast cancer (MOA-MB-453 and MB231), melanoma (G361, G32TG, A875), a thyroid cancer (TTC11), a gastric cancer (KATO3), esophageal cancer (ECGI10), a pancreatic cancer (ASPC1) and a lung cancer cell lines (A549). The cells were cultured in the RPMI-1640 medium (Nissui Pharmaceutical Co. Ltd., Tokyo) with 10% fetal bovine serum and 50 μg/ml penicillin/streptomycin at humidified 5% CO_2/95% air at 37°C.

Primary culture of newborn mouse superior cervical ganglion cells. The SCG neurons were isolated from newborn mice, and treated with 50 ng/ml of NGF for 5 days, as previously reported (14). RNAs were isolated 12, 24, and 48 h after depleting NGF and adding anti-NGF antibody (1% v/v).

Northern blot analysis. Multiple Tissue Northern blot purchased from Clontech (Palo Alto, CA, USA) was used for Northern analysis with cDNA fragments labeled with α-[^{32}P]dCTP as probes. Hybridization was performed in the ExpressHyb hybridization buffer (Clontech) at 68°C for 1 h. Membrane was washed twice in 2X SSC/0.05% SDS at room temperature for 30 min, twice in 0.1X SSC/0.1% SDS at 50°C for 40 min. After washing, the filter was autoradiographed with X-ray film. The membrane was boiled in 0.1% SDS for 10 min for reprobing, and rehybridized with ß-actin as a control.

Semi-quantitative RT-PCR. cDNA was synthesized from 5 μg of total RNA in a 20 μl reaction mixture containing 200 units of Superscript II reverse transcriptase (Life Technologies, Inc.) and pd$(N)_6$ random hexamer (Takara Shuzo Co., Ltd., Ohtsu, Japan). The resulting cDNA fragments were diluted to be a 1:10 solution for PCR templates. The following pairs of forward and reverse primer sets were prepared for amplification: *NLRR-1*, 5'-GTCGATGTCCATGAATACAAC CT-3' and 5'-CAAGGCTAATGACGGCAAAC-3'; *NLRR-2*, 5'-TGACCTATTCCTGACGG-3' and 5'-AAATCACAGTCT CGGGC-3'; *NLRR-3*, 5'-ACTCTTGCCTAATACCCTGAC-3' and 5'-AGATGGTATTCGAGCACTTTG-3'; *GAPDH*, 5'-CTGCACCAACAATATCCC-3' and 5'-GTAGAGACA GGGTTTCAC-3'. All PCR amplifications were performed with a Perkin-Elmer Corp. GeneAmp PCR 9700, using rTaq polymerase (Takara Shuzo Co., Ltd.) with 35 cycles of sequential denaturation (95°C for 15 sec) and annealing-extension (58°C for 15 sec and 72°C for 1 min). *GAPDH* was used as a control and amplified under the same condition except for reduced amplification cycles to 28. PCR templates

were standardized by its *GAPDH* expression before performing semi-quantitative PCR. The products were electrophoresed on 2.0% agarose gels and stained with ethdium bromide for visualization.

Quantitative real-time RT-PCR. cDNA was prepared by the same method as in the semi-quantitative RT-PCR and 2 µl of the 40-fold dilution was used for each PCR reaction. Primers and TaqMan probes for *Nbla10449* and *Nbla10677* were designed using the primer design software Primer Express™ (Perkin-Elmer Applied Biosystems). TaqMan GAPDH control reagent kit (Perkin-Elmer Applied Biosystems) was used for *GAPDH* expression as a control. Reaction mixture (25 µl), containing 2 µl of cDNA, 1X TaqMan mixture, 0.3 µM forward and reverse primers, and 0.2 µM TaqMan probe were used for PCR. The condition of PCR was as follows: 2 min at 50°C (stage 1), 10 min at 95°C (stage 2), and then 50 cycles of amplification for 15 sec at 95°C and 1 min at 60°C (stage 3).

Statistical analysis. The student's t-tests were used to explore possible associations between *Nbla10449/hNLRR-1* expression and other factors, such as age. Since the values of the *Nbla10449/hNLRR-1* and *Nbla10677/hNLRR-3* expression were skewed, a log transformation was used to achieve the normality when using t-test and Cox regression. The distinction between high and low levels of *Nbla10449* was based on the median value (low, *Nbla10449* <0.31 d.u.; high, Nbla10449 >0.31 d.u.), regardless of tumor stage, *MYCN* copy number, or survival. The distinction between high and low levels of *Nbla10677* was based on the median value (low, *Nbla10677* <1.04 d.u.; high, *Nbla10677*>1.04 d.u.), regardless of tumor stage, *MYCN* copy number, or survival. Kaplan-Meier survival curves were calculated, and survival distributions were compared using the log-rank test. Cox regression models were used to explore associations between *Nbla10449/Nbla10677*, age, *MYCN* copy number, mass screening, tumor origin and survival. Statistical significance was declared if the p value was <0.05. Statistical analysis was performed using Stata 6.0. (Stata Statistical Software: Release 6.0 College Station, Stata Corporation, TX, 1999).

Results

Identification of novel human homologues of NLRR family genes, Nbla10449/hNLRR-1 and Nbla10677/hNLRR-3, and their differential expression between favorable and unfavorable subsets of neuroblastoma. To identify the genes differentially expressed between favorable and unfavorable NBLs, semi-quantitative RT-PCR analyses were performed. Sixteen favorable (F) and 16 unfavorable (UF) NBLs were used as PCR templates after normalization by GAPDH expression. So far, ~1,800 independent genes from the NBL cDNA libraries have been surveyed, resulting in the approximately 300 genes with differential expression between the subsets (8,9). Among them, we found *Nbla10449* and *Nbla10677* genes that are highly homologous to the mouse *NLRR-1* and *NLRR-3* genes, respectively. *Nbla10449/hNLRR-1* was preferentially expressed in UF NBLs, whereas *Nbla10677/hNLRR-3* was highly expressed in F NBLs (Fig. 3A).

Full-length cDNA cloning and structure of human NLRR-1, NLRR-2, NLRR-3 and NLRR-5 genes. We performed sequencing of whole inserts of *Nbla10449* and *Nbla10677* and defined their full-length cDNA sequences. In addition, during the process, we also identified human *NLRR-5* by homology search on the database. Furthermore, the other clone, *Nbla00061*, was found to be the same gene as *GAC1* which we renamed as h*NLRR-2*. *NLRR-4* has recently been reported by another group (15).

Nbla10449/hNLRR-1. A full-length *Nbla10449* genes comprised 3,060 bp, with an open reading frame (ORF) of 2,151 bp. The deduced protein was 716 a.a. in length, and included 2 hydrophobic stretches corresponding to a signal peptide at the extreme N-terminal region and a deduced transmembrane domain close to the C-terminal region (Fig. 1A). Analysis of the extracellular domain revealed the presence of 11 leucine-rich repeats encompassed by flanking cystein cluster, a leucine-rich repeat N-terminal domain (LRRNT) and a leucine-rich repeat C-terminal domain (LRRCT), a single immunogloblin C2 type domain, and a fibronectin type III domain (Fig. 1). Homology search against public database showed that *Nbla10449* was identical to the human *EST KIAA1497* (GenBank/DDBJ accession number AB040930) which lacked the N-terminal region and was similar to 2 leucine-rich repeat proteins, m*NLRR-1* (acc. no. D45913) and *Xenopus* x*NLRR-1* (acc. no. AB014462). The identities of deduced Nbla10449 protein to mNLRR-1 and xNLRR-1 were 92 and 75%, respectively. We also analyzed genomic structure of *Nbla10449*, and found that this gene comprised of single exon without any intron and mapped to chromosome 3p region.

Nbla10677/hNLRR-3. Nbla10677 comprised 2,471 bp with an ORF of 2,127bp (acc. no. AB060967) without intron, and mapped to chromosome 7q31. The deduced protein contained 708 a.a. and had a similar structure to Nbla10449/hNLRR-1 (Fig. 1A). In addition, the RGD sequence, an integrin-binding domain, was found in the leucine-rich repeats. Homology search showed that *Nbla10677* was identical to human cDNA FLJ11129 (acc. no. AK001991) and highly similar to the leucine-rich repeat proteins of mouse (mNLRR-3; acc. no. D49802) and rat (rNLRR-3; acc. no. AF291437). Therefore, Nbla10677 seemed to be a human NLRR-3. The Nbla10677/hNLRR-3 showed 85 and 83% similarity to mNLRR-3 and rNLRR-3 proteins, respectively.

Nbla00061/GAC1/hNLRR-2. The *Nbla00061* cDNA clone comprised 3,206 bp including a partial ORF of 2,142 bp. Sequence analysis revealed that it is identical to a *glioma amplified on chromosome 1* gene, *GAC1* (acc. no. AF030435), mapped to chromosome 1q32.1. The GAC1 protein, which was previously reported to be a member of an NLRR protein family (15), had 713 a.a. with a similar structure to NLRR-1 and 3 (Fig. 1). GAC1 showed 98% identity to mNLRR-2, although the latter was reported as only a partial sequence (16). It showed only 54 and 50% identities to mNLRR-1 and mNLRR-3, respectively, indicating that Nbla00061/GAC1 is a human counterpart of mNLRR-2.

m*NLRR-4* was cloned by another group from hemangioblast-like cell line derived from E11.5 mouse AGM and its predicted protein has 4 LRRs, fibronectin 3 and EGF-like motives in the extracellular region (Rump A *et al*, The Molecular Biology Society of Japan Conference, Yokohama,